



Journal of The Ferrata Storti Foundation

## Chronic lymphocytic leukemia cells impair osteoblastogenesis and promote osteoclastogenesis: role of TNF $\alpha$ , IL-6 and IL-11 cytokines

by Paolo Giannoni, Cecilia Marini, Giovanna Cutrona, Serena Matis, Maria Cristina Capra, Francesca Puglisi, Paola Luzzi, Simona Pigozzi, Gabriele Gaggero, Antonino Neri, Katia Todoerti, Fortunato Morabito, Adalberto Ibatici, Maurizio Miglino, Micaela Bergamaschi, Silvia Bruno, Gian Mario Sambuceti, Jean Louis Ravetti, Manlio Ferrarini, Franco Fais, and Daniela de Toterò

Haematologica 2020 [Epub ahead of print]

*Citation: Paolo Giannoni, Cecilia Marini, Giovanna Cutrona, Serena Matis, Maria Cristina Capra, Francesca Puglisi, Paola Luzzi, Simona Pigozzi, Gabriele Gaggero, Antonino Neri, Katia Todoerti, Fortunato Morabito, Adalberto Ibatici, Maurizio Miglino, Micaela Bergamaschi, Silvia Bruno, Gian Mario Sambuceti, Jean Louis Ravetti, Manlio Ferrarini, Franco Fais, and Daniela de Toterò. Chronic lymphocytic leukemia cells impair osteoblastogenesis and promote osteoclastogenesis: role of TNF $\alpha$ , IL-6 and IL-11 cytokines.*

*Haematologica. 2020; 105:xxx*

*doi:10.3324/haematol.2019.231456*

### *Publisher's Disclaimer.*

*E-publishing ahead of print is increasingly important for the rapid dissemination of science. Haematologica is, therefore, E-publishing PDF files of an early version of manuscripts that have completed a regular peer review and have been accepted for publication. E-publishing of this PDF file has been approved by the authors. After having E-published Ahead of Print, manuscripts will then undergo technical and English editing, typesetting, proof correction and be presented for the authors' final approval; the final version of the manuscript will then appear in print on a regular issue of the journal. All legal disclaimers that apply to the journal also pertain to this production process.*

## **Chronic lymphocytic leukemia cells impair osteoblastogenesis and promote osteoclastogenesis: role of TNF $\alpha$ , IL-6 and IL-11 cytokines.**

Paolo Giannoni<sup>1</sup>, Cecilia Marini<sup>2</sup>, Giovanna Cutrona<sup>3</sup>, Serena Matis<sup>3</sup>, Maria Cristina Capra<sup>3</sup>, Francesca Puglisi<sup>1</sup>, Paola Luzzi<sup>1</sup>, Simona Pigozzi<sup>4</sup>, Gabriele Gaggero<sup>4</sup>, Antonino Neri<sup>5,6</sup>, Katia Todoerti<sup>5</sup>, Fortunato Morabito<sup>7,8</sup>, Adalberto Ibatici<sup>9</sup>, Maurizio Miglino<sup>9</sup>, Micaela Bergamaschi<sup>9</sup>, Silvia Bruno<sup>10</sup>, Gian Mario Sambuceti<sup>11</sup>, Jean Louis Ravetti<sup>4</sup>, Manlio Ferrarini<sup>10</sup>, Franco Fais<sup>3,10</sup>, Daniela de Toter<sup>3\*</sup>.

1: Dept. Experimental Medicine, Biology Section, University of Genoa, Italy

2: CNR institute of Bioimages and Molecular Physiology, Milan, Italy

3: Molecular Pathology Unit, IRCCS-Ospedale Policlinico San Martino, Genoa, Italy

4: Pathological Anatomy Unit, IRCCS-Ospedale Policlinico San Martino, Genoa, Italy

5: Dept. of Oncology and Hemato-Oncology, University of Milan, Italy

6: Hematology Unit Fondazione IRCCS Ca' Granda, Ospedale Maggiore Policlinico, Milan, Italy

7: Biotechnology Research Unit, Azienda Ospedaliera di Cosenza, Aprigliano, Cosenza, Italy

8: Dept. Of Hematology and Bone Marrow transplant, Augusta Victoria Hospital, Jerusalem, Israel

9: Hematology Clinic, IRCCS-Ospedale Policlinico San Martino, Genoa, Italy

10: Dept. of Experimental Medicine, Anatomy Section; University of Genoa, Genoa, Italy

11: Nuclear Medicine Unit, IRCCS-Ospedale Policlinico San Martino, Genoa, Italy

**Running title:** CLL cells affect osteoblasto/osteoclastogenesis

\*Corresponding Author:

Dr. Daniela de Toter PhD; Molecular Pathology Unit, IRCCS-Ospedale Policlinico San Martino, L.go R. Benzi, 10, 16132-Genoa, Italy; Tel:+39 010 555 8973; e-mail: daniela.detotero@hsanmartino.it

Word count abstract: 249; Word count main text: 3989; 8 Figures; 1 Supplementary file

## **Acknowledgments**

Funding was provided by Ricerca Corrente line “Host- Cancer Interaction” (CM, FF); CNR flagship program Interomics 2015 (CM); Associazione Italiana Ricerca sul Cancro (AIRC); 5 x mille n.9980 (to MF, AN) and by AIRC I.G. n.14326 (to MF) and n.15426 (to FF) and 16722, 10136 (to AN); and Compagnia San Paolo, Turin, Italy project 2017 0526 (GC), and Italian Ministry of Health 5x1000 funds 2014 (to GC) and funds 2015 (to FF). Authors would like to thank Dr. S. Zupo for providing supplementary CLL samples.

## **ABSTRACT**

Bone skeletal alterations are no longer considered a rare event in Chronic Lymphocytic Leukemia (CLL), especially at more advanced stages of the disease. This study is aimed at elucidating the mechanisms underlying this phenomenon. Bone marrow stromal cells, induced to differentiate toward osteoblasts in osteogenic medium, appeared unable to complete their maturation upon co-culture with CLL cells, CLL cells-derived conditioned media (CLL-cm) or CLL-sera (CLL-sr). Inhibition of osteoblast differentiation was documented by decreased levels of RUNX2 and osteocalcin mRNA expression, by increased osteopontin and DKK-1 mRNA levels, and by a marked reduction of mineralized matrix deposition. The addition of neutralizing TNF $\alpha$ , IL-11 or anti-IL-6R monoclonal antibodies to these co-cultures resulted into restoration of bone mineralization, indicating the involvement of these cytokines: these findings were further supported by silencing TNF $\alpha$ , IL-11 and IL-6 in leukemic cells. We also demonstrated that the addition of CLL-cm to monocytes, previously stimulated with MCSF and RANKL, significantly amplified the formation of large mature osteoclasts as well as their bone resorption activity. Moreover enhanced osteoclastogenesis, induced by CLL-cm, was significantly reduced by treating cultures with the anti-TNF $\alpha$  moAb Infliximab; an analogous effect was observed by the use of the BTK inhibitor Ibrutinib. CLL cells, co-cultured with mature osteoclasts, were interestingly protected from apoptosis and upregulated Ki-67. These experimental results parallel the direct correlation between TNF $\alpha$  amounts in CLL sera and the degree of compact bone erosion we previously described, further strengthening the indication of a reciprocal influence between leukemic cells expansion and bone structure derangement.

## INTRODUCTION

In Chronic Lymphocytic Leukemia (CLL) patients' skeletal erosion can be demonstrated by TC-scan at the level of long bone shafts and in subjects with a more advanced disease (Binet C versus Binet A).<sup>(1, 2)</sup> Moreover a few number of CLL/SLL cases show osteolysis along with hypercalcemia.<sup>(3-7)</sup> Axial bone structure alterations appear also more frequent in CLL patients than in age matched controls.<sup>(8)</sup> Bone erosion mechanisms in CLL patients are however not elucidated so far, and may be part of a complexity of events participating to disease pathogenesis. Recent evidence demonstrated that mutual interactions between stromal and leukemic cells facilitate survival and expansion of the neoplastic clone<sup>(9-13)</sup> and contemporarily affect functions of microenvironmental cells. We previously described a direct correlation between the levels of RANKL (nuclear factor-kB ligand) expression on CLL cells and the degree of bone erosion in CLL patients<sup>(2)</sup>.

We suggested that leukemic cells, progressively infiltrating bone marrow (BM), may affect osteoblasts and osteoclasts differentiation, finally leading to alterations of physiological bone remodeling. RANKL, expressed by osteoblasts, is the major cytokine regulating osteoclasts differentiation after binding to RANK+ monocytes. In Multiple Myeloma (MM) osteolytic bone lesions are considered a hallmark and malignant plasma cells show high RANKL expression and secretion; here the interactions between malignant plasma cells, releasing RANKL, and bone microenvironment progressively undermine the integrity of bone structures due to stimulation of osteoclasts activity and subsequent excessive bone resorption.<sup>(14-16)</sup> RANKL is expressed at high levels also in malignant CLL cells but, at difference with MM cells, CLL cells release it only in exceptional cases.<sup>(17)</sup> Indeed Borge et al. detected high amounts of plasmatic RANKL in one CLL patient displaying lytic bone lesions (800 pg/mL) and demonstrated that leukemic B cells, *in vitro*, release high RANKL levels (1600 pg/mL) after CPG stimulation.<sup>(3)</sup> However RANKL stimulation induces the production of pro-osteoclastic cytokines, such as TNF $\alpha$ , IL-6 and IL-8 by CLL cells.<sup>(17, 18)</sup> Therefore several growth factors may contribute to the microenvironment/leukemic B cells cross-talks ruling bone homeostasis.

Based on these premises we investigated whether cytokines secreted by leukemic cells participate to bone alterations in CLL patients. Some evidences, collected here, indicate that released CLL cytokines prevent the osteoblast-induced bone formation and contemporarily stimulate the expansion of osteoclasts progenitors or of fully mature osteoclasts. Altogether these observations suggest that the disruption of the physiological bone marrow niche may create favorable

conditions for CLL cells expansion: relevant to this notion is the proof that survival/expansion of leukemic cells appears promoted by activated osteoclasts.

## **METHODS**

This study was approved by the IRCCS Ospedale Policlinico San Martino Ethic Committee, Genoa, Italy. 45 patients were included in the study (Binet Stages: 19A, 17B and 9C). MEC-1 cells (DSMZ Cell Line Collection) were used in selected experiments. Details for all Methods are provided in the Supplementary file.

### **Osteoblasts generation.**

Bone marrow stromal cells (BMSC), previously expanded,<sup>(12)</sup> were osteogenically induced, co-cultured with CLL B cells (contact/transwell), CLL cell conditioned media (CLL-cm) or CLL sera (CLL-sr) for 5 more days (Supplementary Fig. 1), detached and processed.

### **Messenger RNA extraction, reverse transcription and quantitative real time RT-PCR.**

Real time RT-PCR assessed expression of GAPDH, Osteopontin (OP), Osteocalcin (OC), RUNX2, Dickkopf-1 (DKK-1), Cathepsin K (Cat-K), NFATc-1 and Matrix Metalloproteinase 9 (MMP9).

### **Evaluation of matrix deposition.**

Alizarine staining was performed on para-formaldehyde-fixed cultures of osteo-induced BMSC, under different treatments, by a commercial kit.

### **Short-interfering RNA-mediated knock-down of specific cytokines in MEC-1 or CLL cells**

All short-interfering RNAs (siRNA: IL-6-, IL-11-, TNF $\alpha$ -specific or aspecific) used were commercially available.

### **Osteoclasts generation.**

Monocytes purified from PBMCs of healthy donors or from CLL patients were induced to differentiate toward osteoclasts and then cultured under different conditions (Supplementary Fig. 1): CLL-cm with/without neutralizing anti-cytokine/receptor moAbs, Ibrutinib, Denosumab, or from cytokine-silenced CLL cells.

### **TRAP Staining and Bone resorption Assay.**

Tartrate-resistant acid phosphatase (TRAP) detection was performed by a commercial kit. Osteoclast activity was evaluated by sizing resorption pits produced in an inorganic crystalline material.

### **Viability and cell cycle evaluation of CLL B cells co-cultured with osteoclasts.**

14-days-derived-osteoclasts were co-cultured with CLL cells and apoptosis of leukemic cells was determined through DiOC6 staining<sup>(19)</sup> or by Propidium Iodide (PI) cell cycle-phase distribution through multiparameter flow cytometric analysis.<sup>(20)</sup> Ki-67 expression was also determined by flow cytometry.

### **Immuno-histochemical analyses of bone biopsies.**

B5-fixed, decalcified and paraffin-embedded tissue blocks were sectioned, de-paraffinized and rehydrated. Endogenous peroxidase was blocked with 5% H<sub>2</sub>O<sub>2</sub>; serial sections were immunostained for TRAP and CD79a.

### **Detection of TNF $\alpha$ levels in media recovered from CLL cells, cultured alone or with osteo-induced BMSC, and in sera of CLL cells-engrafted-mice.**

Human TNF $\alpha$  levels in media from osteo-induced BMSC and CLL cells were determined by Millipore's Milliplex KIT. We further determined human TNF $\alpha$  levels in sera of mice displaying a documented bone loss after human CLL cells engraftment.<sup>(2)</sup>

### **TNF $\alpha$ , IL-11 and IL-6 detection in CLL-cm.**

TNF $\alpha$  amounts in co-cultures of monocytes, differentiating toward osteoclasts under various conditions (MCSF+RANKL, MCSF+RANKL+CLL-cm or MCSF+CLL-cm only), were assessed through a qualitative Elisa assay and compared. TNF $\alpha$ , IL-11 or IL-6 in conditioned media of CLL-cm, *per se* or upon cytokine-knock down, were determined by the same approach.

### **GEP analysis.**

B cells from CLL samples and normal PBL were profiled on GeneChip Gene 1.0 ST Array.<sup>(21)</sup>

**Statistics.**

Two-sided Student *t*-test, U-Mann-Whitney test, or  $\chi^2$  test with Fisher's correction were used. All used data sets displayed a normal distribution; p values are depicted as \*, \*\* or \*\*\* for  $p \leq 0.05$ ,  $\leq 0.01$  or  $< 0.001$ , respectively.

## RESULTS

### **Osteo-induced BMSC are inhibited in their terminal differentiation by addition of CLL cells, CLL-conditioned media or CLL-sera.**

Normal donors BMSC were induced to differentiate toward osteoblasts and then co-cultured with CLL cells (contact/transwell), CLL-conditioned media (CLL-cm) or CLL-sera (CLL-sr) (Supplementary Fig. 1A). After 5 days of co-culturing, osteo-induced BMSC were evaluated for RUNX2, osteocalcin, Dickkopf-1 (DKK1) and osteopontin mRNAs levels by quantitative RT-PCR. RUNX2, the master gene regulating the osteoblastogenic cascade, appeared significantly down-regulated by the presence of CLL cells, CLL-cm or CLL-sr, but not by normal B cells (Fig. 1). Osteocalcin, normally high in fully differentiated osteoblasts, was also significantly reduced. DKK-1, a canonical WNT inhibitor, appeared instead highly upregulated with a clear trend in all the experimental conditions. Osteopontin mRNA was also enhanced, although even by normal B cells. Altogether these findings indicate that CLL cells affect the expression of the major osteoblasts-related genes and inhibit differentiation of BMSC towards osteoblasts.

### **Reduced extracellular matrix deposition by osteo-induced BMSC cultured with CLL cells, CLL-conditioned media or CLL sera.**

The inhibition of osteoblasts differentiation by CLL cells was also confirmed through the evaluation of matrix mineralization levels. Through Alizarine Red staining, mineralized areas appeared consistently reduced, the strongest inhibition of matrix deposition being in the presence of CLL-cm or CLL-sr (Fig. 2A, B). Based on literature data<sup>(22-24)</sup> we investigated whether IL-6, IL-11 and TNF $\alpha$  could represent candidate cytokines mediating osteoblast differentiation inhibition. The effect of an anti-GP130 moAb was also tested because this molecule, shared among the different cytokines of the IL-6 family, is pivotal in signal transduction. Monoclonal antibodies neutralizing the above mentioned cytokines (IL-11, TNF $\alpha$ ) or blocking binding to their receptors (IL-6R, GP130) were thus added, together with CLL-cm, to cultures of osteo-induced BMSC. All these moAbs, but not an isotype specific control (Supplementary Fig. 2A), counteracted suppression of *in vitro* mineralized matrix deposition, significantly higher after Infliximab addition (Fig. 2C, D). Cultures of osteo-induced BMSC with conditioned media from TNF $\alpha$ -, IL-6-, or IL-11-RNA-silenced MEC-1 cell line or primary leukemic cells (BA101), further confirmed involvement of these cytokines in osteoblast differentiation impairment (Fig. 2E, F, G, H and Supplementary Fig. 2A-B). Moreover the increase

in mineralized matrix deposition, detected in osteo-induced BMSC cultured with CLL cm + neutralizing moAbs, was paralleled by the restoration of higher levels of RUNX2 and osteocalcin mRNAs (Supplementary Fig. 2C, D). Evidences of a decreased pSTAT3<sup>(ser727)</sup> and AKT expression, in CLL-cm-treated BMSC versus CLL-cm + Infliximab or in basal conditions, suggest the participation of these signaling pathways to the regulation of osteogenesis by CLL-released TNF $\alpha$  (Supplementary Figure 2E, F).

The observations of a higher mRNA expression for IL-11 and IL-11 receptor A (IL-11RA) in CLL cells than in control B cells, by GEP analysis, highlight IL-11 as a CLL cells-released cytokine (Supplementary Fig. 4). An association between increased levels of IL-6 produced by CLL cells and worse clinical outcomes has been further recently reported.<sup>(25)</sup> The substantial amounts of TNF $\alpha$ , present in conditioned media derived from CLL cells cultured alone (basal conditions: Control), but significantly reduced in media from CLL/BMSC co-cultures (Supplementary Fig. 5), suggest that TNF $\alpha$ , constitutively secreted by CLL cells and metabolically active, plays a role in suppressing osteoblasts differentiation.

#### **Enhancement of differentiation of allogeneic or autologous monocytes into osteoclasts by CLL cells conditioned media.**

Next, we investigated whether the presence of CLL-cm could affect osteoclastogenic differentiation of monocytes *in vitro*. Purified and pre-activated monocytes, from peripheral blood of healthy donors or of CLL patients, were challenged with CLL-cm, or medium only, for 7 days (Supplementary Fig. 1). The osteoclasts number, evaluated by counting the number of TRAP<sup>+</sup> cells with three or more nuclei, significantly increased after the addition of CLL-cm (Fig. 3A, C). Moreover osteoclasts derived under this condition appeared larger than those in control cultures, fully differentiated and characterized by multiple nuclei: a canonical ruffle border was sometimes evident (Fig. 3B). The enhancement in osteoclasts differentiation was also detectable when the same experiment was performed in an autologous setting (Fig. 3D-E). A considerable reduction in the number of large multinucleated cells was however observed when monocytes were stimulated without RANKL in the induction phase (MCSF+CLL-cm only). Under this condition, a consistent number of tri-nucleated TRAP<sup>+</sup> cells appeared drastically smaller, in comparison to osteoclasts present in controls cultures derived with exogenous RANKL. We were thus prompted to evaluate the relative proportions of TRAP<sup>+</sup> tri-nucleated small or large cells. Figures 4A and B show that, while pre-stimulation of monocytes with MCSF+RANKL, with/without CLL-cm, led to their

complete maturation, inducing an higher number of typical multinucleated osteoclasts, the addition of MCSF+CLL-cm alone failed to achieve the same effect, consistently impairing the generation of large osteoclasts (Fig. 4C and Supplementary Fig. 6). Low levels of soluble RANKL, found in media derived from cultured CLL cells ( $n=10$ ; data not shown), could thus promote initial osteoclast differentiation only. It is however evident that factors released by CLL cells synergize with RANKL, when exogenously added, thus causing a significant amplification of osteoclastogenesis. This observation appears also sustained by the findings that Cathepsin K, MMP9, NFATc1, pivotal in osteoclasts differentiation, show a higher mRNA expression in monocytes stimulated with MCSF+RANKL and CLL-cm than in monocytes treated with MCSF+RANKL only (Fig. 4D). A statistically significant reduction was also observed in Cathepsin K transcript levels when the culture condition included CLL-cm but was devoid of RANKL (Fig. 4E).

#### **Osteoclasts derived in the presence of MCSF+RANKL and CLL-cm show higher bone resorption activity.**

We then observed that only large fully differentiated and multinucleated osteoclasts, derived after MCSF+RANKL stimulation, show significant bone resorption activity and larger erosion areas were detected when CLL-cm was concomitantly added in these cultures (Fig. 5A-C). Small tri-nucleated cells, generated with MCSF+CLL-cm only, although TRAP<sup>+</sup>, produced very small detectable erosion pits (Fig. 5B). Similar results were obtained when an increased number of RANKL<sup>+</sup> CLL cells (from  $1 \times 10^6$  to  $2 \times 10^6$ /well) were added with MCSF, in the place of the conditioned medium, attempting to compensate for soluble RANKL lack. Implementation of seeded monocyte numbers (from  $1.3 \times 10^5$ /well to  $2.6 \times 10^5$ /well), cultured with MCSF+CLL-cm, also failed to give rise to mature osteoclasts fully competent in matrix erosion. The ability of eroding bone appears therefore in strict relationship with the presence of fully and large differentiated osteoclasts, characterized by a typical sealing zone. Nurse-like cells, tumor associated macrophages (TAM) typically found in the CLL microenvironment<sup>(11, 26)</sup>, although TRAP<sup>+</sup>, were also devoid of resorbing bone surface activity (Fig. 5D).

#### **Involvement of TNF $\alpha$ , IL-6 and IL-11 in enhanced osteoclast maturation by CLL-cm.**

To assess whether TNF $\alpha$ , IL-6 and IL-11 could be involved in enhanced formation of osteoclasts by CLL-cm, we added neutralizing moAbs for TNF $\alpha$ , IL-11 or anti-IL-6R, -GP130 moAbs to cultures of monocytes stimulated with MCSF+CLL-cm, with/without previous RANKL activation. Anti-IL-6R and

anti-IL-11 moAbs reduced monocytes osteoclastogenesis in the absence of RANKL pre-stimulation only, while the anti-GP-130 acted also in the presence of RANKL (Fig. 6A). Infliximab (anti-TNF $\alpha$ ), instead, inhibited differentiation of large multinucleated osteoclasts, previously activated with MCSF+RANKL (Fig. 6B, C). Altogether these observations suggest that IL-6 and IL-11 drive monocytes toward an initial stage of osteoclast maturation, while TNF $\alpha$ , in synergy with RANKL, plays a key role in the differentiation of fully competent multinucleated osteoclasts. Conditioned media from TNF $\alpha$ -silenced MEC-1 cells weakly decreased the formation of large osteoclasts and increased the number of small trinucleated TRAP $^+$  cells (Supplementary Fig. 7). Higher levels of TNF $\alpha$  were also detected in media recovered from MCSF+RANKL-activated monocytes, cultured in the presence of CLL-cm, than in all the other experimental conditions (Fig. 6D). Data derived from experiments in the CLL mouse model, which results in derangement of bone structure following leukemic cells engraftment <sup>(2)</sup>, appears in line with these observations. Moreover TNF $\alpha$  levels, found in mouse sera but of human source, appeared increased from the 3<sup>rd</sup> to the 6<sup>th</sup> weeks, after CLL cells injection (Supplementary Fig. 8). Collectively these observations suggest that TNF $\alpha$  may have a key role in impairment of the physiological bone remodeling in CLL patients. Of note, the concentration of TNF $\alpha$  in sera directly correlated with the degree of bone erosion in CLL patients.<sup>(2)</sup>

### **Osteoclasts support CLL viability *in vitro*.**

To investigate whether osteoclasts support leukemic cells viability we generated fully differentiated osteoclasts and then co-cultured them with CLL cells, while measuring apoptosis during time course experiments. Osteoclasts significantly prevented CLL cells from spontaneous apoptosis (Fig. 7A). Interestingly also small TRAP $^+$  tri-nucleated cells, derived by treating monocytes with MCSF and CLL-cm, without RANKL, displayed analogous effects (Fig. 7B). Bright field images of Fig. 7C depict viable leukemic B cells surrounding large classical osteoclasts or smaller osteoclasts precursors in *in vitro* co-culture. While assessing whether osteoclasts could stimulate CLL cells proliferation, we determined that, after osteoclasts co-culture, Ki-67 was up-regulated on the whole leukemic population but scored markedly positive in a limited fraction of cells (Ki-67 bright: Fig. 7D-E). Accordingly, only a limited number of cells was induced by the osteoclasts to progress through cell cycle along the experimental timings (Fig. 7F).

### **Bone biopsies from CLL patients show the presence of small and large TRAP<sup>+</sup> osteoclasts.**

The presence of osteoclasts was further addressed in bone marrow biopsies from two CLL patients. Classical large cells, immuno-challenged for TRAP positivity, appeared in close contact with bone trabeculae, but much smaller TRAP<sup>+</sup> cells were also detectable (Fig. 8A); the formers, canonical and differentiated osteoclasts, were located on bone surfaces, while the latter, activated TRAP<sup>+</sup> monocytes possibly representing immature osteoclasts, were mostly observable within the bone marrow stroma of the biopsies (Fig. 8A, row A). Moreover, in co-immuno staining experiments, CD79a<sup>+</sup> leukemic B cells often appeared in strict vicinity of large TRAP<sup>+</sup> cells (Fig. 8A, row B), further indicating that direct cross-talks between the two cell types may take place *in vivo*. Additionally, as shown in figure 8B, the number of osteoclasts found in bone biopsies from 3 CLL patients appeared higher than in normal controls.

### **Ibrutinib inhibits increased osteoclastogenesis induced by CLL-cm.**

BCR-tyrosine kinases inhibitors, such as the BTK inhibitor Ibrutinib, represent the gold standard therapy for CLL patients. BTK, a member of the TEC kinases family, integrates RANK/RANKL and ITAM pathways along osteoclasts formation and activity.<sup>(27)</sup> We determined that Ibrutinib significantly inhibited the enhanced generation of large mature osteoclasts when contemporarily added with CLL-cm to previously activated monocyte cultures (Supplementary Fig. 9). Ibrutinib treatment may thus counteract survival stimuli provided by the bone microenvironment.

## DISCUSSION

In recent years it has become increasingly clear that the bi-directional cross-talk<sup>(28)</sup> between CLL cells and cellular components of the microenvironment plays a relevant role in disease progression. We have here demonstrated that CLL cells affect the differentiation of the two major bone components: osteoblasts and osteoclasts. Indeed CLL cells, through the release of soluble factors, on one side inhibit osteoblasts differentiation and on the other increase osteoclastogenesis and bone resorption. TNF $\alpha$ , IL-6 and IL-11 appear involved in the inhibition of osteoblasts differentiation: cytokines knock-down, the use of neutralizing moAbs or blocking binding to their receptors significantly counteracted the inhibition of extracellular matrix deposition when osteo-induced BMSC are cultured in the presence of CLL-cm. Restoration in bone matrix deposition, particularly evident after the addition of the anti-TNF $\alpha$  moAb Infliximab, suggests a major role of TNF $\alpha$  in the CLL cells-driven impairment of osteoblastogenesis. Indeed TNF $\alpha$  affects osteoblasts function and differentiation through the inhibition of the production of extracellular matrix components (*i.e.* type I collagen), or down-modulating the expression of osteocalcin and alkaline phosphatase.<sup>(29)</sup> TNF $\alpha$  also inhibits the expression of the osteoblast differentiation factor RUNX2.<sup>(30)</sup> Accordingly, neutralization of TNF $\alpha$  in CLL-cm rescued levels of RUNX2 and Osteocalcin mRNA in osteo-induced BMSC, paralleling matrix mineralization increase. Moreover a contribution of pSTAT3 and AKT, as downstream molecules involved in bone remodeling signals<sup>(31)</sup> by leukemic cells, may be envisaged through decreased levels of these molecules in BMSC treated with CLL-cm only, as compared with TNF $\alpha$ -neutralized CLL-cm. Interestingly gene expression profile analysis of *in silico* available datasets<sup>(32)</sup> highlights that, in human MSC, different molecules, involved in regulation of the osteoblast differentiation, become modulated after CLL cells co-culture: a descending trend for RUNX2 and a significant decrease in the expression of Collagen 1A, BMP-4 and BMP-6, along with an increase in DKK-1 and Osteopontin have been in fact demonstrated (Supplementary Fig. 10). These observations further point to interactive cross-talks between CLL cells and MSC possibly leading to niche modifications. Suppression of osteoblasts differentiation by leukemic cells has been reported in ALL, CML and in MM<sup>(33-35)</sup> through alteration of NOTCH signaling pathway.

It is also known that TNF $\alpha$  stimulates bone resorption.<sup>(36, 37)</sup> In our model TNF $\alpha$ , acting in synergism with RANKL, increased differentiation of fully multinucleated osteoclasts and Infliximab significantly blocked the enhancement in the formation of fully mature osteoclasts treated with

CLL-cm. This finding suggests that TNF $\alpha$ , released by leukemic cells, stimulates osteoclastogenesis. As previously reported, malignant CLL cells release TNF $\alpha$  <sup>(38)</sup>, and the levels of plasmatic TNF $\alpha$ , higher in CLL patients than in healthy controls, correlate with disease stage, CD38 expression and chromosomal abnormalities (17p and 11q deletion).<sup>(39)</sup> Interestingly TNF $\alpha$  levels, significantly higher in sera from patients with advanced disease than in patients with stable disease (Binet C vs Binet A:  $n=36$  cases studied), are in direct proportion with the degree of appendicular bone erosion.<sup>(2)</sup> Among CLL patients enrolled in our osteoclastogenesis studies, we further determined a direct correlation between TNF $\alpha$  serum levels and the unmutated IGVH status of the assessed patients (serum cut-off level: 9.0 pg/mL;  $\chi^2$  test,  $p=0.0046$ ). We also evidenced that the same unmutated IGVH status of the CLL cell donors correlated with an increased number of trinucleated TRAP $^+$  cells when pre-activated monocytes are cultured with their CLL-derived cm ( $\chi^2$  test,  $p=0.0147$ ; Supplementary Fig. 11).

TNF $\alpha$  has a key role in many inflammatory diseases characterized by bone damage and enhanced osteoclasts differentiation (rheumatoid arthritis or in psoriatic arthritis).<sup>(40-42)</sup> It has been recently demonstrated that the TNF $\alpha$ -promoted osteoclastogenesis is exerted solely in the contemporary presence of RANKL <sup>(43)</sup>, as we also evidenced. Other cytokines released by leukemic cells, such as IL-6 and IL-11, may however contribute to monocyte differentiation and participate to the redundancy of the osteoclastogenesis control. In the absence of RANKL pre-stimulation, neutralizing anti-IL-11 or the anti-IL-6R or-GP130 moAbs reduced the number of small trinucleated TRAP $^+$  cells derived from monocytes cultured with MCSF and CLL-cm only. Hence cytokines present in CLL-cm (*i.e.* IL-6, IL-11) might prompt monocytes toward an early step of osteoclast differentiation, thus stimulating the expansion of precursor cells: low levels of soluble RANKL may further limit their ability to complete osteoclast differentiation. Observations from McCoy et al.<sup>(44)</sup> appear in accord with this suggestion: although IL-11 derived from breast tumor promoted the development of osteoclast progenitors, the enhancement of fully differentiated osteoclasts appeared however dependent onto subsequent RANKL addition. MCP1 also, when provided alone, increased differentiation of monocytes in multinuclear TRAP $^+$  cells without bone resorption activity. Nonetheless the same cells, after RANKL exposure, differentiated into authentic bone resorbing osteoclasts.<sup>(45)</sup> The complex process of osteoclasts differentiation involves the regulated expression of various molecules and their linked transduced signal. The interaction between RANKL, residing on osteoblasts, and RANK, expressed on activated monocytes, results in the recruitment of tumor necrosis factor (TNF) receptor-associated factor-6

(TRAF-6) which in turn activates NF- $\kappa$ B, JNK, ERK, p38, Akt and NFATc1. In particular NFATc1 is considered the master transcription factor that regulates the expression of molecules like MMP9, OSCAR, DC stamp, TRAP and Cathepsin K, which altogether define the functional osteoclast phenotype.<sup>(46)</sup> We have shown here higher Cathepsin K, MMP9, and NFATc1 mRNA expression in RANKL-activated monocytes cultured with CLL-cm than in controls: this finding may parallel the observed increment in the number of fully differentiated osteoclasts found after CLL-cm addition. The reduced levels of mRNA Cathepsin K observed in monocytes stimulated with CLL-cm only may further suggest a blockade of their differentiative stage.

High incidence of bone alterations, in various B cell malignancies (BCM) including CLL, has been previously reported.<sup>(47)</sup> In BCM osteo-biopsies, a consistent number of TRAP<sup>+</sup> monocytes are located near bone trabeculae and characterized by a size smaller than osteoclast found in MM. These small cells induced areas of micro-resorption and are in proximity of malignant lymphoid cells. Further evidences of the presence of minute single bytes facing small TRAP<sup>+</sup> osteoclasts in BCM eroded bone surfaces were subsequently provided.<sup>(48)</sup> These findings suggest that, in BCM, higher numbers of active small osteoclasts are needed to cause rates of resorption similar to those observed in MM patients. The evaluation of the frequency distribution profile of the osteoclasts dimensions in BCM bone sections has interestingly demonstrated the existence of a bimodal distribution of TRAP<sup>+</sup> osteoclasts, characterized by two different average diameters, peaking at 10-15  $\mu$ m and at 20-25  $\mu$ m. In MM, instead, the distribution appeared homogenous and uni-modal, with a single peak around 20-25  $\mu$ m.<sup>(49)</sup> Data obtained from our *in vitro* model of osteoclasts generation, under different conditions, resemble these *in vivo* findings: consistent numbers of small tri-nucleated TRAP<sup>+</sup> cells and only limited numbers of large mature osteoclasts could be derived when MCSF-activated monocytes were cultured with CLL-cm alone. On the contrary, pre-stimulation with RANKL allowed the differentiation of monocytes in authentic fully mature osteoclasts. Bone structure alterations might be therefore relatively common in CLL patients, but usually surmised, because extensive bone lesions do not frequently occur. Reasonably, in CLL patients, the multi-cytokine panel produced by leukemic cells stimulates the generation of osteoclast progenitors which, however, usually fail to reach a complete maturation. Hence the impaired bone homeostasis in CLL differs from what previously determined in MM: in the former malignant plasma cells release RANKL, while in the latter CLL cells are incapable of shedding it.<sup>(17)</sup> Exceptionally some CLL cases, hypothetically characterized by more advanced disease stage and possibly by the presence of higher levels of RANKL and TNF $\alpha$ , might display osteolysis. Presence of

neoplastic B often close to osteoclasts appears also of interest <sup>(50)</sup>: small areas of bone micro-resorption could represent small niches of recovery and protection for neoplastic B cells. We confirmed that in bone biopsies from CLL patients, leukemic cells are detectable in strict vicinity of osteoclasts, thus suggesting their mutual interactions. The proof that fully differentiated osteoclasts, or their precursors, protect leukemic B cells from apoptosis, up-regulate Ki-67 and stimulate their proliferation sustains the idea of an active interplay between these two cell populations. Moreover the disruption of CLL cells-mediated osteoclasts support by the BTK inhibitor Ibrutinib, is a novel undisclosed finding. Finally the observations from the present study highlight new relationships between neoplastic CLL cells and normal bone counterparts, evidence a mutually-active alteration of the local pathological marrow microenvironment and suggest a widened perspective for novel therapeutic targets.

**Author's contribution:**

DdT and PG designed the experiments, analyzed data and wrote the paper, DdT, PG, MCC, FP, PL, SM, SP, SB, GG, KT performed the experiments; AI, MB, MM, GC, FF, JLR, FM, CM, GMS, AN, MF contributed materials and advice.

## REFERENCES

1. Fiz F, Marini C, Piva R, et al. Adult advanced chronic lymphocytic leukemia: computational analysis of whole-body CT documents a bone structure alteration. *Radiology*. 2014;271(3):805-813.
2. Marini C, Bruno S, Fiz F, et al. Functional Activation of Osteoclast Commitment in Chronic Lymphocytic Leukaemia: a Possible Role for RANK/RANKL Pathway. *Sci Rep*. 2017;7(1):14159.
3. Borge M, Delpino MV, Podaza E, et al. Soluble RANKL production by leukemic cells in a case of chronic lymphocytic leukemia with bone destruction. *Leuk Lymphoma*. 2016;57(10):2468-2471.
4. Hua J, Ide S, Ohara S, et al. Hypercalcemia and osteolytic bone lesions as the major symptoms in a chronic lymphocytic leukemia/small lymphocytic lymphoma patient: a rare case. *J Clin Exp Hematop*. 2018;58(4):171-174.
5. Katz H, Sagun S, Griswold D, Alsharedi M. Solitary Lytic Bone Metastasis: A Rare Presentation of Small Lymphocytic Leukemia. *Case Rep Hematol*. 2018;2018:6154709.
6. McMillan P, Mundy G, Mayer P. Hypercalcaemia and osteolytic bone lesions in chronic lymphocytic leukaemia. *Br Med J*. 1980;281(6248):1.
7. Soni P, Aggarwal N, Rai A, et al. Chronic Lymphocytic Leukemia: A Rare Cause of Pathological Fracture of the Femur. *J Invest Med High Impact Case Rep*. 2017;5(4):1-3.
8. Olszewski AJ, Gutman R, Eaton CB. Increased risk of axial fractures in patients with untreated chronic lymphocytic leukemia: a population-based analysis. *Haematologica*. 2016;101(12):e488-e491.
9. Burger JA, Gandhi V. The lymphatic tissue microenvironments in chronic lymphocytic leukemia: in vitro models and the significance of CD40-CD154 interactions. *Blood*. 2009;114(12):2560-2561; author reply 2561-2562.
10. Burger JA, Ghia P, Rosenwald A, Caligaris-Cappio F. The microenvironment in mature B-cell malignancies: a target for new treatment strategies. *Blood*. 2009;114(16):3367-3375.
11. Giannoni P, Pietra G, Travaini G, et al. Chronic Lymphocytic Leukemia Nurse-like cells express the hepatocyte growth factor receptor (c-MET) and indoleamine 2,3-dioxygenase and display features of immunosuppressive type 2 skewed macrophages. *Haematologica*. 2014;99(6):2-11.

12. Giannoni P, Scaglione S, Quarto R, et al. An interaction between hepatocyte growth factor and its receptor (c-MET) prolongs the survival of chronic lymphocytic leukemic cells through STAT3 phosphorylation: a potential role of mesenchymal cells in the disease. *Haematologica*. 2011;96(7):1015-1023.
13. Lagneaux L, Delforge A, Bron D, De Bruyn C, Stryckmans P. Chronic lymphocytic leukemic B cells but not normal B cells are rescued from apoptosis by contact with normal bone marrow stromal cells. *Blood*. 1998;91(7):2387-2396.
14. Bataille R, Chappard D, Marcelli C, et al. Mechanisms of bone destruction in multiple myeloma: the importance of an unbalanced process in determining the severity of lytic bone disease. *J Clin Oncol*. 1989;7(12):1909-1914.
15. Roodman GD. Pathogenesis of myeloma bone disease. *Leukemia*. 2009;23(3):435-441.
16. Valentin-Opran A, Charhon SA, Meunier PJ, Edouard CM, Arlot ME. Quantitative histology of myeloma-induced bone changes. *Br J Haematol*. 1982;52(4):601-610.
17. Schmiedel BJ, Scheible CA, Nuebling T, et al. RANKL expression, function, and therapeutic targeting in multiple myeloma and chronic lymphocytic leukemia. *Cancer Res*. 2013;73(2):683-694.
18. Secchiero P, Corallini F, Barbarotto E, et al. Role of the RANKL/RANK system in the induction of interleukin-8 (IL-8) in B chronic lymphocytic leukemia (B-CLL) cells. *J Cell Physiol*. 2006;207(1):158-164.
19. De Totero D, Meazza R, Zupo S, et al. Interleukin-21 receptor (IL-21R) is up-regulated by CD40 triggering and mediates proapoptotic signals in chronic lymphocytic leukemia B cells. *Blood*. 2006;107(9):3708-3715.
20. Bruno S, Ghiotto F, Tenca C, et al. N-(4-hydroxyphenyl)retinamide promotes apoptosis of resting and proliferating B-cell chronic lymphocytic leukemia cells and potentiates fludarabine and ABT-737 cytotoxicity. *Leukemia*. 2012;26(10):2260-2268.
21. Morabito F, Mosca L, Cutrona G, et al. Clinical monoclonal B lymphocytosis versus Rai 0 chronic lymphocytic leukemia: A comparison of cellular, cytogenetic, molecular, and clinical features. *Clin Cancer Res*. 2013;19(21):5890-5900.
22. Hughes FJ, Turner W, Belibasakis G, Martuscelli G. Effects of growth factors and cytokines on osteoblast differentiation. *Periodontol 2000*. 2006;41:48-72.
23. Manolagas SC. The role of IL-6 type cytokines and their receptors in bone. *Ann N Y Acad Sci*. 1998;840:194-204.

24. Sims NA. Cell-specific paracrine actions of IL-6 family cytokines from bone, marrow and muscle that control bone formation and resorption. *Int J Biochem Cell Biol.* 2016;79:14-23.
25. Wang HQ, Jia L, Li YT, Farren T, Agrawal SG, Liu FT. Increased autocrine interleukin-6 production is significantly associated with worse clinical outcome in patients with chronic lymphocytic leukemia. *J Cell Physiol.* 2019;234(8):13994-14006.
26. Burger JA, Tsukada N, Burger M, Zvaifler NJ, Dell'Aquila M, Kipps TJ. Blood-derived nurse-like cells protect chronic lymphocytic leukemia B cells from spontaneous apoptosis through stromal cell-derived factor-1. *Blood.* 2000;96(8):2655-2663.
27. Shinohara M, Koga T, Okamoto K, et al. Tyrosine kinases Btk and Tec regulate osteoclast differentiation by linking RANK and ITAM signals. *Cell.* 2008;132(5):794-806.
28. Ding W, Nowakowski GS, Knox TR, et al. Bi-directional activation between mesenchymal stem cells and CLL B-cells: implication for CLL disease progression. *Br J Haematol.* 2009;147(4):471-483.
29. Gowen M, MacDonald BR, Russell RG. Actions of recombinant human gamma-interferon and tumor necrosis factor alpha on the proliferation and osteoblastic characteristics of human trabecular bone cells in vitro. *Arthritis Rheum.* 1988;31(12):1500-1507.
30. Gilbert L, He X, Farmer P, et al. Expression of the osteoblast differentiation factor RUNX2 (Cbfa1/AML3/Pebp2alpha A) is inhibited by tumor necrosis factor-alpha. *J Biol Chem.* 2002;277(4):2695-2701.
31. Zhou H, Newnum AB, Martin JR, et al. Osteoblast/osteocyte-specific inactivation of Stat3 decreases load-driven bone formation and accumulates reactive oxygen species. *Bone.* 2011;49(3):404-411.
32. Schulze-Edinghausen L, Durr C, Ozturk S, et al. Dissecting the Prognostic Significance and Functional Role of Progranulin in Chronic Lymphocytic Leukemia. *Cancers.* 2019;11(6):822.
33. Delgado-Calle J, Anderson J, Cregor MD, et al. Bidirectional Notch Signaling and Osteocyte-Derived Factors in the Bone Marrow Microenvironment Promote Tumor Cell Proliferation and Bone Destruction in Multiple Myeloma. *Cancer Res.* 2016;76(5):1089-1100.
34. Kumar A, Anand T, Bhattacharyya J, Sharma A, Jaganathan BG. K562 chronic myeloid leukemia cells modify osteogenic differentiation and gene expression of bone marrow stromal cells. *J Cell Commun Signal.* 2018;12(2):441-450.
35. Mangolini M, Ringshausen I. Bone Marrow Stromal Cells Drive Key Hallmarks of B Cell Malignancies. *Int J Mol Sci.* 2020;21(4):1466.

36. Bertolini DR, Nedwin GE, Bringman TS, Smith DD, Mundy GR. Stimulation of bone resorption and inhibition of bone formation in vitro by human tumour necrosis factors. *Nature*. 1986;319(6053):516-518.
37. Nanes MS. Tumor necrosis factor-alpha: molecular and cellular mechanisms in skeletal pathology. *Gene*. 2003;321:1-15.
38. Foa R, Massaia M, Cardona S, et al. Production of tumor necrosis factor-alpha by B-cell chronic lymphocytic leukemia cells: a possible regulatory role of TNF in the progression of the disease. *Blood*. 1990;76(2):393-400.
39. Ferrajoli A, Keating MJ, Manshour T, et al. The clinical significance of tumor necrosis factor-alpha plasma level in patients having chronic lymphocytic leukemia. *Blood*. 2002;100(4):1215-1219.
40. Colucci S, Brunetti G, Cantatore FP, et al. Lymphocytes and synovial fluid fibroblasts support osteoclastogenesis through RANKL, TNFalpha, and IL-7 in an in vitro model derived from human psoriatic arthritis. *J Pathol*. 2007;212(1):47-55.
41. Dimitroulas T, Nikas SN, Trontzas P, Kitas GD. Biologic therapies and systemic bone loss in rheumatoid arthritis. *Autoimmun Rev*. 2013;12(10):958-966.
42. Fantuzzi F, Del Giglio M, Gisondi P, Girolomoni G. Targeting tumor necrosis factor alpha in psoriasis and psoriatic arthritis. *Expert Opin Ther Targets*. 2008;12(9):1085-1096.
43. Luo G, Li F, Li X, Wang ZG, Zhang B. TNFalpha and RANKL promote osteoclastogenesis by upregulating RANK via the NFkappaB pathway. *Mol Med Rep*. 2018;17(5):6605-6611.
44. McCoy EM, Hong H, Pruitt HC, Feng X. IL-11 produced by breast cancer cells augments osteoclastogenesis by sustaining the pool of osteoclast progenitor cells. *BMC Cancer*. 2013;13:16.
45. Kim MS, Day CJ, Selinger CI, Magno CL, Stephens SR, Morrison NA. MCP-1-induced human osteoclast-like cells are tartrate-resistant acid phosphatase, NFATc1, and calcitonin receptor-positive but require receptor activator of NFkappaB ligand for bone resorption. *J Biol Chem*. 2006;281(2):1274-1285.
46. Amarasekara DS, Yun H, Kim S, Lee N, Kim H, Rho J. Regulation of Osteoclast Differentiation by Cytokine Networks. *Immune Netw*. 2018;18(1):e8.
47. Marcelli C, Chappard D, Rossi JF, et al. Histologic evidence of an abnormal bone remodeling in B-cell malignancies other than multiple myeloma. *Cancer*. 1988;62(6):1163-1170.

48. Chappard D, Rossi JF, Bataille R, Alexandre C. Osteoclast cytomorphometry and scanning electron microscopy of bone eroded surfaces during leukemic disorders. *Scanning Microsc.* 1990;4(2):323-328.
49. Chappard D, Rossi JF, Bataille R, Alexandre C. Osteoclast cytomorphometry demonstrates an abnormal population in B cell malignancies but not in multiple myeloma. *Calcif Tissue Int.* 1991;48(1):13-17.
50. Rossi JF, Chappard D, Marcelli C, et al. Micro-osteoclast resorption as a characteristic feature of B-cell malignancies other than multiple myeloma. *Br J Haematol.* 1990;76(4):469-475.

## Legends to Figures

### **FIGURE 1: The addition of CLL conditioned media, CLL sera or CLL cells to osteo-induced BMSC impairs their differentiation.**

The addition of CLL conditioned medium (cm), CLL sera (sr) or CLL cells, in contact (co) or in transwell (tw), to cultures of BMSC, induced to differentiate in standard osteogenic medium, inhibits their complete differentiation toward osteoblasts. RUNX2 and Osteocalcin transcript levels resulted significantly decreased. DKK-1 and Osteopontin mRNA were instead increased when CLL-cm, CLL-sr or CLL cells were added in the cultures, as compared with control BMSC cultured with osteogenic medium only. Given the extremely high average and corresponding SD values of DKK-1 mRNA levels, statistical significance was not achieved for CLL-cm and CLL-sr treatment. The mRNA expression of the same genes of interest has been also evaluated in co-cultures of B purified from normal controls (B ctrl); *n* indicates the number of cases examined for each experimental conditions.

### **FIGURE 2: The addition of CLL conditioned media, CLL sera or CLL cells to osteo-induced BMSC impairs mineralized matrix deposition as revealed by Alizarine Red staining.**

**A** and **B**: When CLL conditioned media (cm), CLL sera (sr) or CLL cells, in contact (co) or in transwell (tw), were added to BMSC induced to differentiate in standard osteogenic medium a reduced deposition of mineralized matrix was detected. This effect was particularly and significantly evident in the presence of CLL-cm or CLL-sr ( $p < 0.001$ ). **C** and **D**: The inhibition of mineralized matrix deposition, due to the addition of CLL-cm derived from 4 CLL patients (FW16, LSA01, MS15, MAO2), was counteracted by neutralizing anti-TNF $\alpha$ , -IL-11 moAbs or anti-IL-6R, -GP130 moAb. The anti-TNF $\alpha$  moAb Infliximab showed a higher efficiency in restoring mineralization. **E** and **F**: The addition of conditioned medium (cm) derived from cultures of IL-6-, IL-11-, TNF $\alpha$ -silenced MEC-1 cells or leukemic CLL cells (BA101) restored mineralization by osteo-induced BMSC, as shown in a representative well of two assessed; in parallel neutralizing moAbs for the same cytokines rescued matrix mineralization, as shown in **G** and **H**. Histogram bars depict the percentage of Alizarine-positive area of each well.

**FIGURE 3: Enhancement of osteoclasts differentiation following the addition of CLL conditioned media to cultures of monocytes, from healthy donors or CLL patients, pre-stimulated with MCSF+RANKL.**

**A:** The addition of CLL conditioned medium (cm) enhances osteoclasts differentiation of healthy monocytes pre-stimulated with MCSF and RANKL, as shown here with cm from a representative case (cm FW16). The number of osteoclasts has been determined by counting the number of TRAP<sup>+</sup> cells, at least tri-nucleated. **B:** Osteoclasts generated with the addition of CLL-cm show a typical morphology of multinucleated (N) large cells with a ruffle border (RF) **C:** The addition of CLL-cm derived from CLL cell cultures of different patients (BE08, CRO7, JF1h2, FW16, BE117, MG37, VG34) to monocytes purified from 3 healthy donors (1310, 1363, 1610) significantly increases the differentiation of monocytes, previously stimulated with MCSF+RANKL, toward osteoclasts. **D and E:** CLL-cm from the SD36 CLL patient was added to autologous monocytes, previously stimulated with MCSF+RANKL: also in this autologous setting condition a significant enhancement of osteoclasts differentiation was observable. For 10X, 20X or 40X depicted images bar sizes are 25, 12.5 or 6.25 $\mu$ m, respectively.

**FIGURE 4: Evaluation of the size of osteoclasts derived from monocytes cultured with MCSF and CLL-cm in the presence or absence of RANKL, and of the mRNA expression of key molecules involved in this process.**

**A and B:** TRAP<sup>+</sup> cells, at least tri-nucleate and derived in the presence of MCSF+CLL-cm ( $n=3$ ; FA35, SD36, TC38) show a size smaller than osteoclasts classically derived with MCSF+RANKL or MCSF+RANKL+CLL-cm. **C:** Size distribution of osteogenically induced monocytes with MCSF+RANKL or MCSF+CLL-cm. The curves depict the percentages of cells that fall within the limits of each class size (square pixels) **D:** Cathepsin K, MMP9 and NFAT-C1 mRNA are higher in osteoclasts derived with CLL-cm. **E:** The levels of Cathepsin K mRNA expression is significantly higher in osteoclasts derived with CLL-cm in the presence of RANKL than without RANKL.

**FIGURE 5: The addition of CLL-cm enhances the resorption activity of MCSF+RANKL derived osteoclasts.**

**A:** Osteoclasts derived in the presence of CLL-cm show a significant enhancement in bone resorption activity in comparison with controls derived with only MCSF+RANKL. Images are representative of two different experiments with CLL-cm derived from 3 CLL patients. **B:**

Osteoclasts derived in the presence of MCSF+CLL-cm, without RANKL pre-activation, show instead a few pits of resorption. NLCs, although TRAP<sup>+</sup>, do not resorb bone. Images are representative of two experiments **C**: The addition of CLL-cm to MCSF-RANKL pre-stimulated monocytes significantly increases the osteoclasts ability to resorb the bone; *n*: number of visual fields assessed within two different experiments and CLL-cm derived from 3 CLL patients. **D**: Increasing the number of seeded monocytes ( $1.3 \times 10^5$  or  $2.6 \times 10^5$ /well) stimulated with MCSF only does not result in enhanced resorption activity. Increasing the number of CLL cells ( $1 \times 10^6$  or  $2 \times 10^6$ /well) expressing RANKL on their surface was also not sufficient to compensate for lack of soluble RANKL; *n*: number of visual fields assessed within two experiments. Nurse-like cells (NLC) also do not display bone resorbing activity

**FIGURE 6: Anti-IL-11 or anti-IL-6R moAbs reduce the differentiation of osteoclast precursors. Infliximab (anti-TNF $\alpha$ ) inhibits the generation of mature authentic osteoclasts derived in the presence of RANKL. Higher levels of TNF $\alpha$  were in parallel detected in culture media of monocytes pre-stimulated with RANKL and then with CLL-cm**

**A**: Neutralization of IL-11 and of IL-6 inhibits the differentiation of TRAP<sup>+</sup> tri-nucleated cells derived in the presence of MCSF+CLL-cm (M+cm), putatively representing osteoclast precursors, but not of those reaching terminal differentiation, derived in the presence MCSF+RANKL+CLL-cm (MR+cm). Anti-GP130 moAb affect both the number of putative precursors and mature osteoclasts. Large and small indicates the size of the cells as defined in Fig. 4. Values are derived from three different experiments and three CLL cases. **B**: TNF $\alpha$ , added in cultures of MCSF+RANKL-pre-activated healthy monocytes, stimulates the number of differentiated osteoclasts which also appear larger than in controls. The addition of CLL-cm from one CLL patient (MAO2) enhances osteoclasts formation, while the neutralizing anti-TNF $\alpha$  moAb markedly reduces the enhanced osteoclastogenesis observed. Size bar: 25 $\mu$ m **C**: Histograms depict the number of large and small osteoclasts derived in the presence of CLL-cm, with/without neutralizing anti-TNF $\alpha$  moAb, from five different CLL cases, as assayed in different experiments. Infliximab addition markedly reduced the number of large fully differentiated osteoclasts. **D**: The amount of TNF $\alpha$  is increased in cultures of monocytes pre-activated with MCSF+RANKL (MR) and then with CLL-cm (MR+cm).

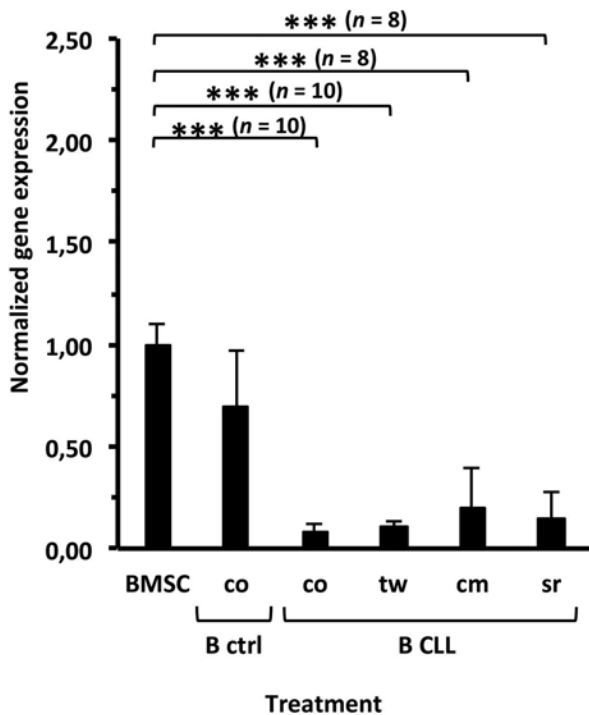
**FIGURE 7: Fully differentiated osteoclasts, as well as osteoclast precursors, support CLL cell survival. A limited number of CLL cells further up-regulate Ki-67 and reactivate cycling after osteoclasts co-culture**

**A:** CLL cells apoptosis was prevented by co-culturing leukemic cells with fully mature osteoclasts for 24h to 7 days (n=8 CLL cases at each time point); **B:** Apoptosis of CLL cells was prevented after their co-culture with osteoclasts derived from healthy monocytes stimulated with MCSF+RANKL, with MCSF+RANKL+CLL-cm or with MCSF+CLL-cm only (putative osteoclasts precursors) as well. Percentage of apoptosis was evaluated by DiOC6 staining after 7 days of co-culture. **C:** Brightfield images show the viability of CLL cells co-cultured with fully differentiated osteoclasts derived in the presence of RANKL (with/without CLL-cm addition) or with osteoclasts precursors derived in the presence of MCSF+CLL-cm only. **D:** Ki-67 was up-regulated on CLL cells after their co-culture with mature osteoclasts (n=4 CLL cases examined). **E:** Ki-67 appeared brightly expressed on a limited number of cells. Ki-67+ leukemic cells progressively increased from 72h to 7 days (1%-15%) **F:** A small population of CLL cells was stimulated to enter in S and G<sub>2</sub>M phases after their co-culture with osteoclasts. CLL cells were stimulated with CPG as controls (n=4 cases analyzed), AVG: average.

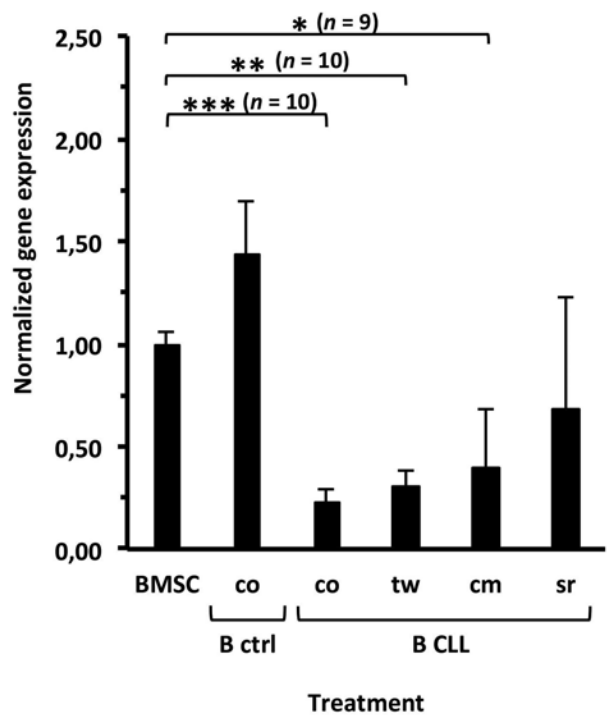
**FIGURE 8: Typical TRAP<sup>+</sup> large osteoclasts and also TRAP<sup>+</sup> cells with a smaller size are present in osteo-biopsies from CLL patients.**

**A,** row A: Large TRAP<sup>+</sup> cells (brown; red arrows) were observed on trabeculae rims (B) while smaller TRAP<sup>+</sup> cells were detectable in the marrow stroma (BM). Representative images from two CLL patients (LSA01, DA06) are shown; row B: TRAP and CD79a co-immunostainings showed that TRAP<sup>+</sup> osteoclast (brown) are often proximal to CD79a<sup>+</sup> leukemic B cells (pink), as displayed in the enlargements; row C: positive controls for TRAP immune-staining: 2 patients with Multiple Myeloma and Myelofibrosis, respectively. Bar size is 125 μm except for the inserts where bars are 32μm. **B:** Number of TRAP<sup>+</sup> osteoclasts, related to the number of bone trabeculae, as observed in bone biopsies sections from 3 CLL patients (LSA01, DA06, BS13) one Multiple Myeloma patient and one normal control. Among CLL patients LSA01 and DA06 were IGVH unmutated and in Binet stage B and C, respectively, while BS13 was in Binet stage C.

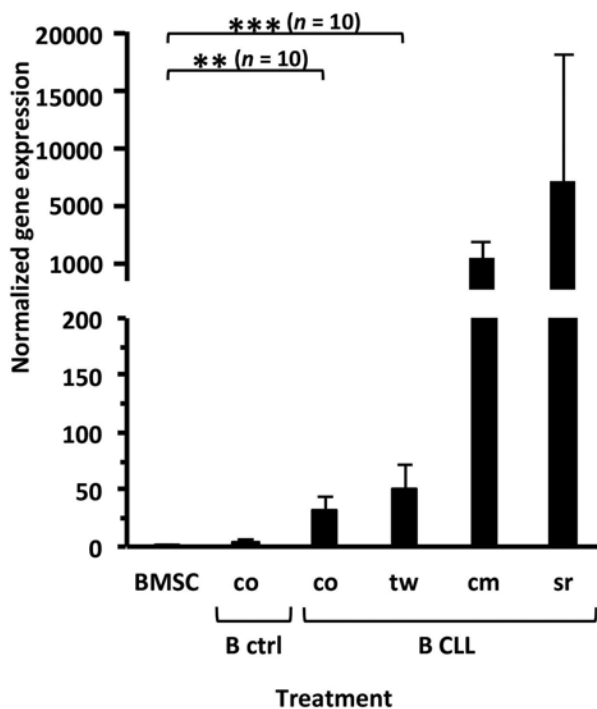
### RUNX-2/GAPDH



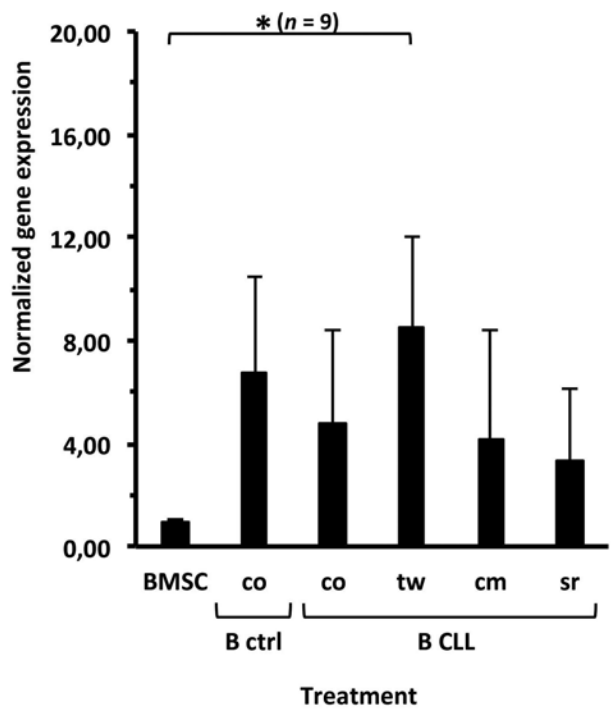
### OSTEOCALCIN/GAPDH

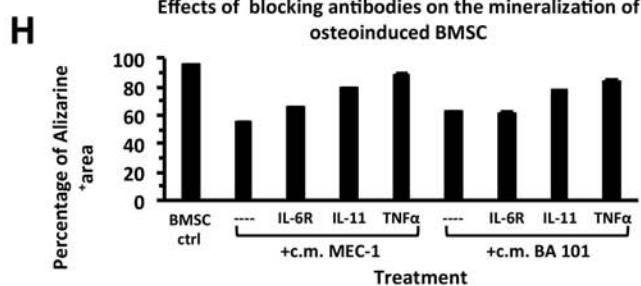
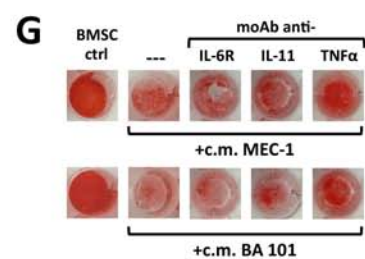
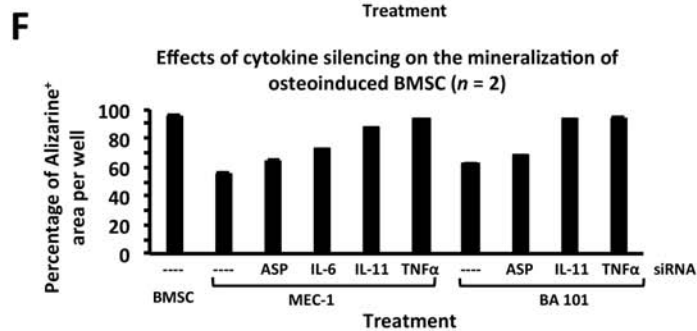
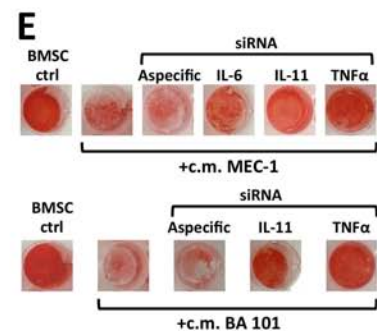
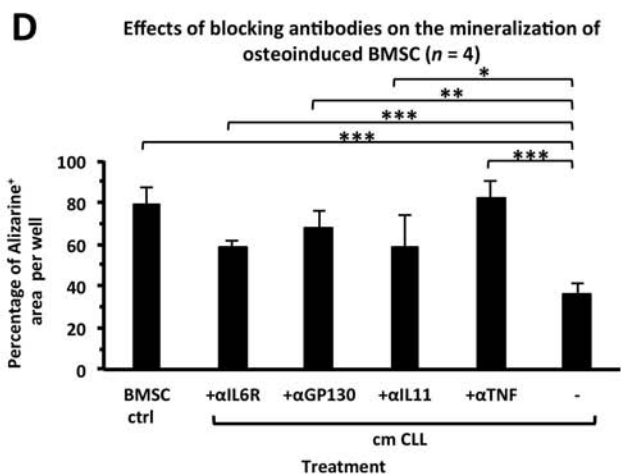
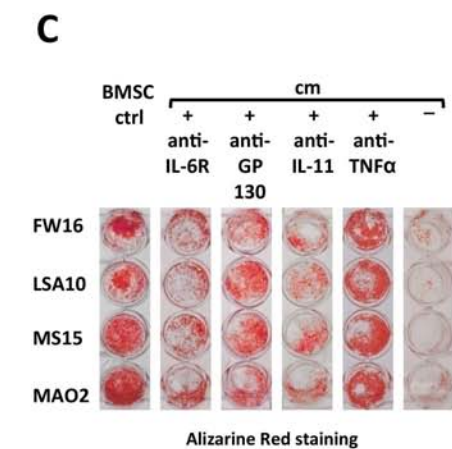
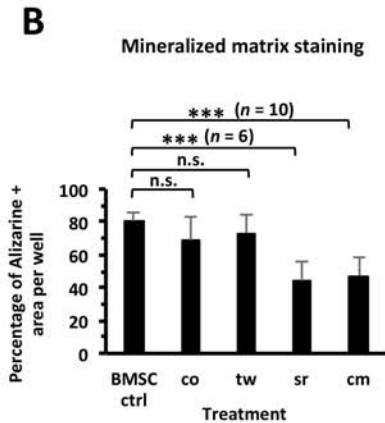
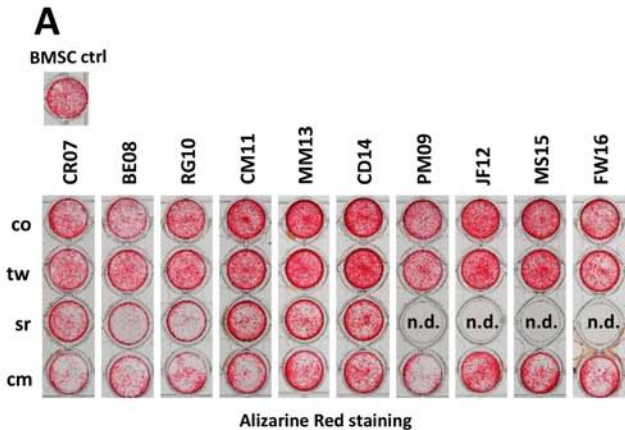


### DKK-1/GAPDH



### OSTEOPONTIN/GAPDH

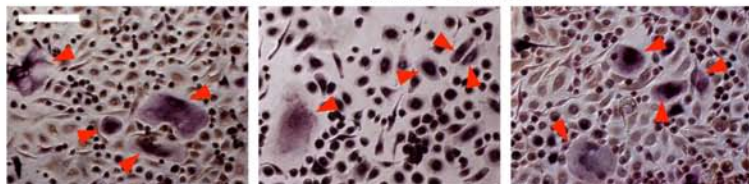




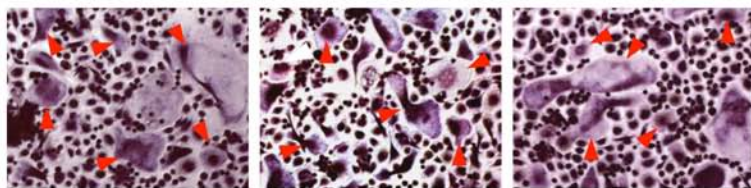
**A**

10x

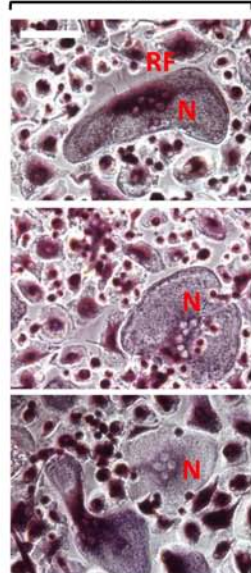
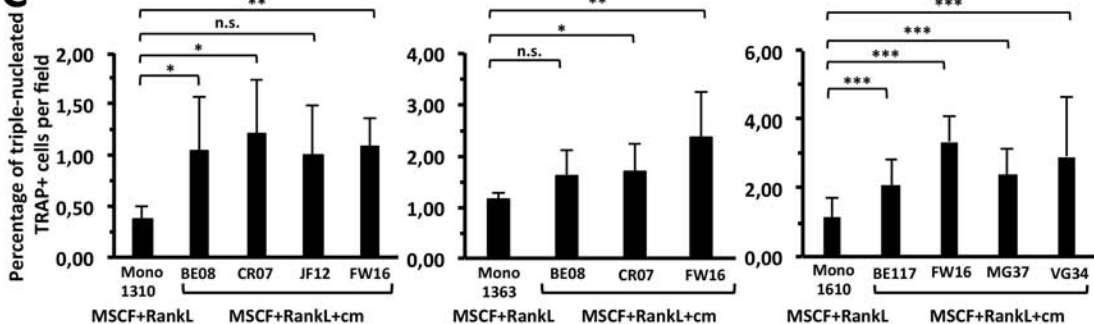
Mono 1610 +MCSF +RANKL



Mono 1610 +MCSF +RANKL +cm FW16

**B**

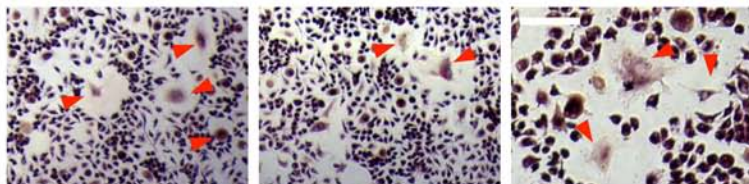
40x

**C****D**

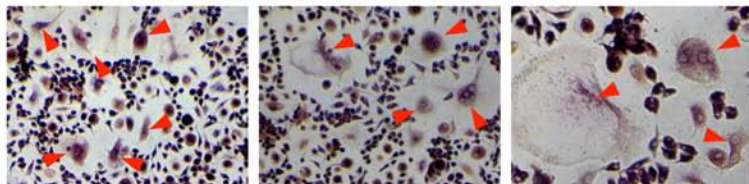
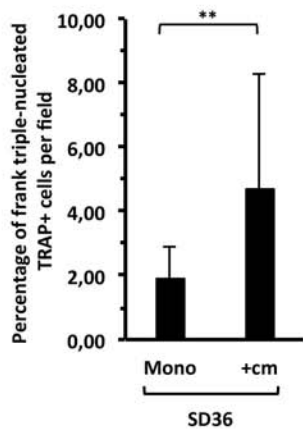
10x

20x

Mono SD36+MCSF+RANKL

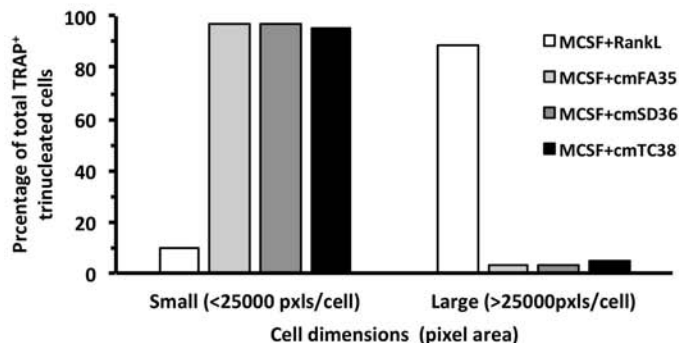
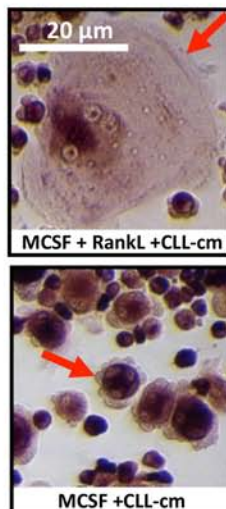


Mono SD36 +MCSF+RANKL + cm SD36

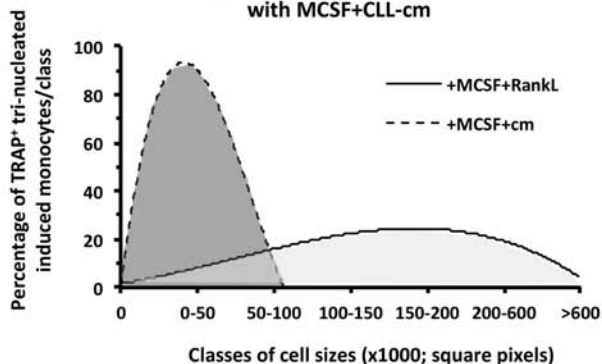
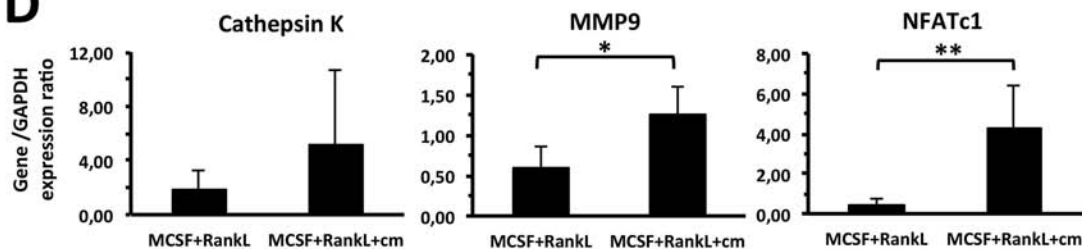
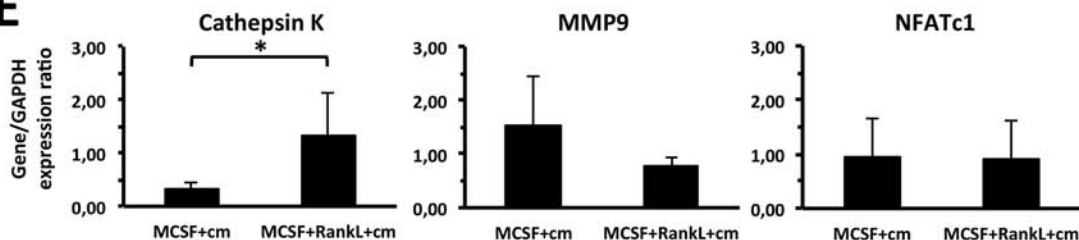
**E**

**A**

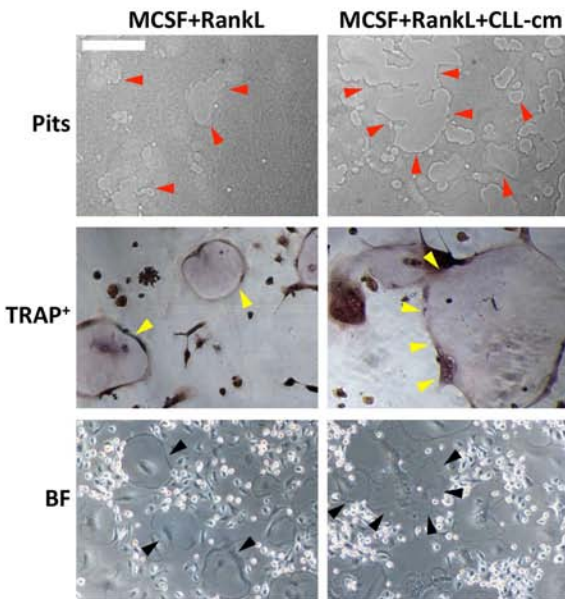
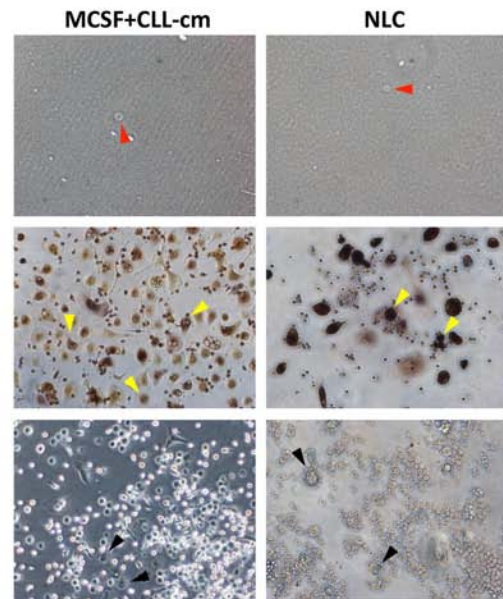
The absence of RankL pre-activation precludes the formation of large fully-differentiated osteoclasts

**B****C**

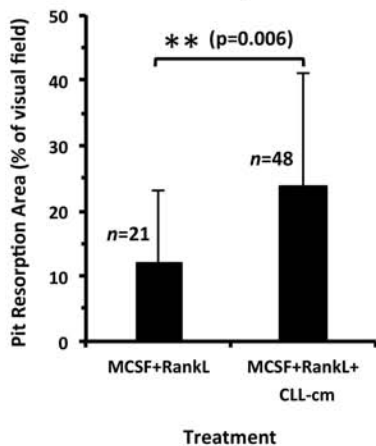
Size distribution comparison between monocytes osteoclastogenically induced with MCSF+RankL or with MCSF+CLL-cm

**D****E**

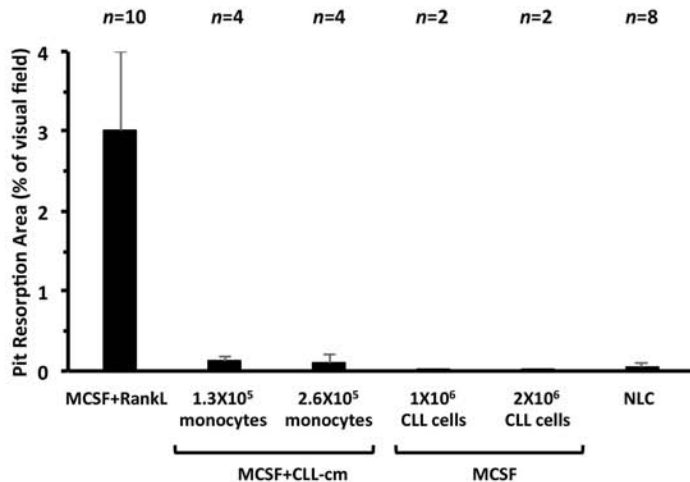
Culture condition

**A****B****C**

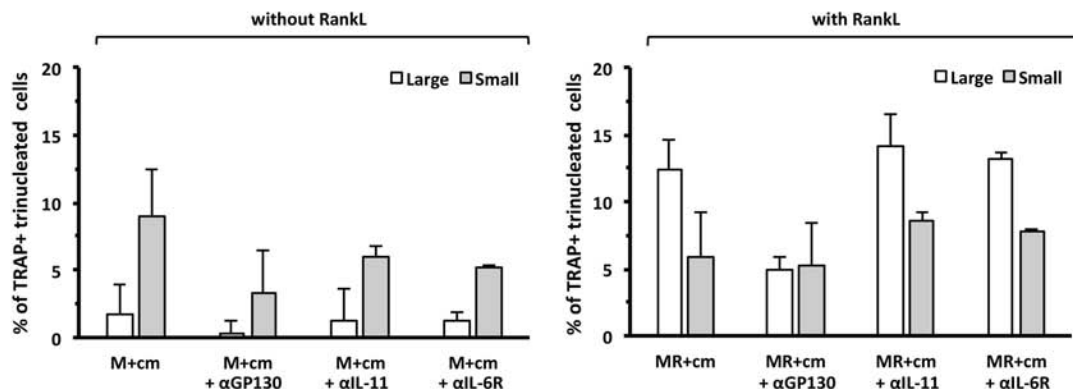
Bone resorption activity of osteoclastogenesis-induced monocytes

**D**

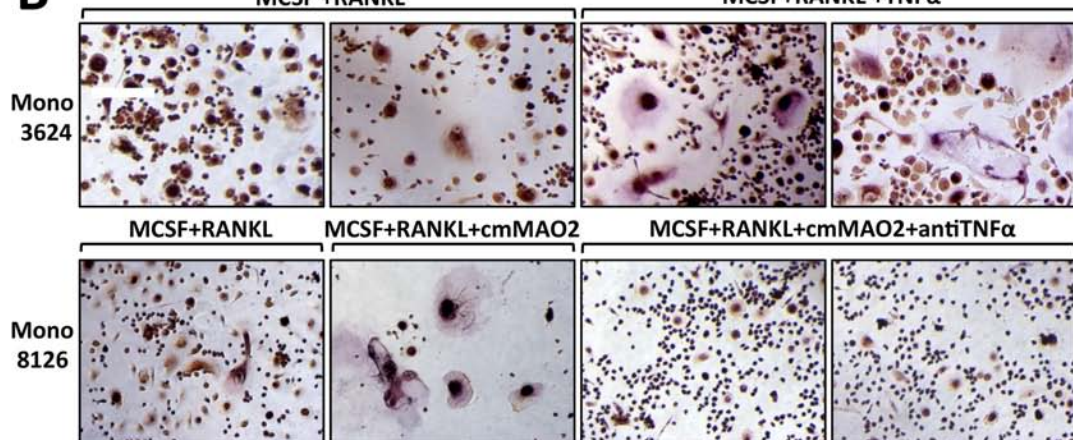
Bone resorption activity of monocytes cultured under different conditions



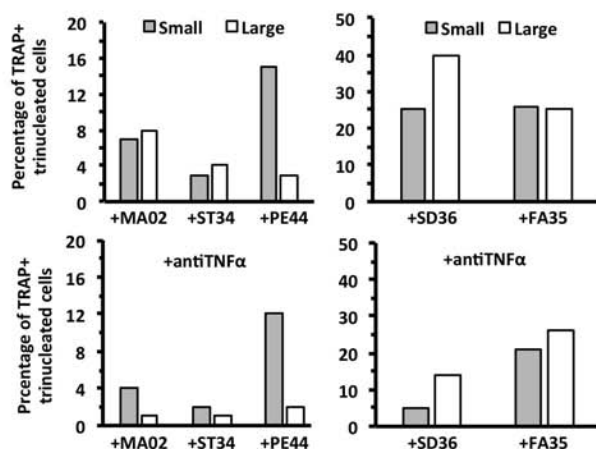
## A Effects of blocking antibodies onto osteoclastogenesis of monocytes cultured with CLL-cm



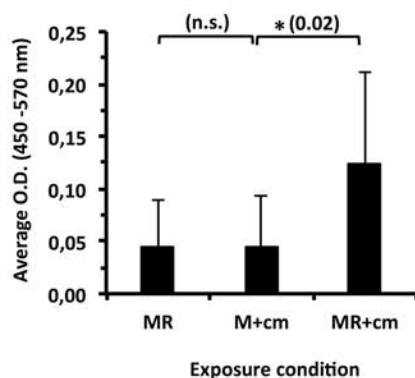
## B MCSF +RANKL MCSF+RANKL +TNF $\alpha$

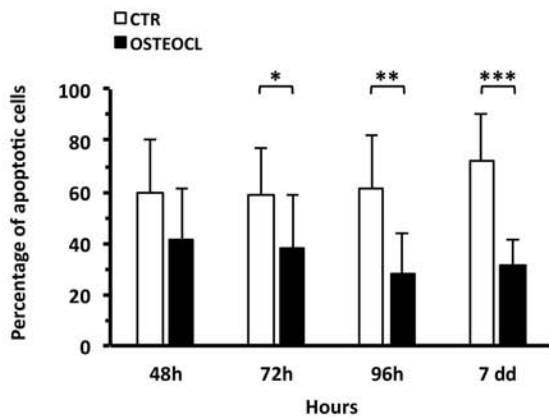
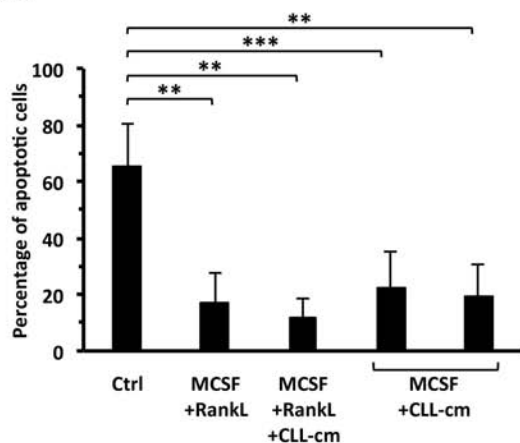
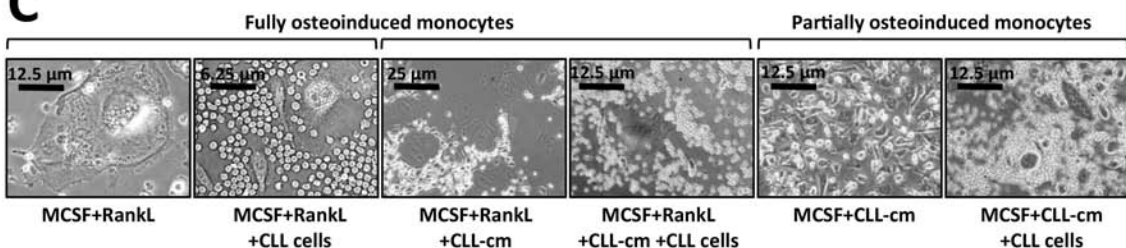
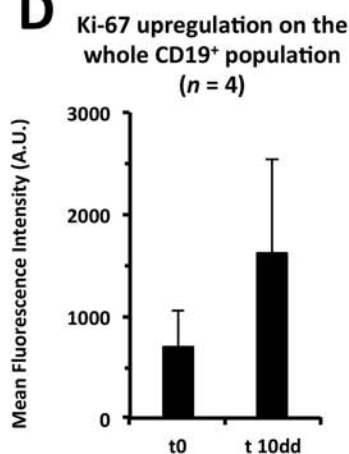
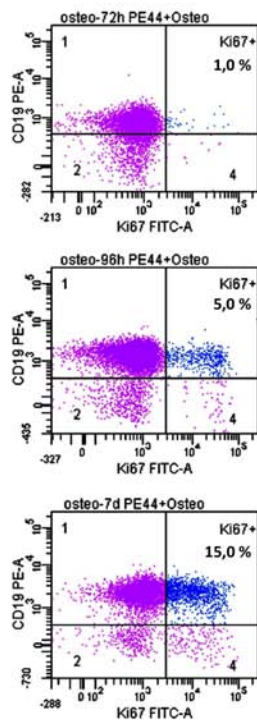
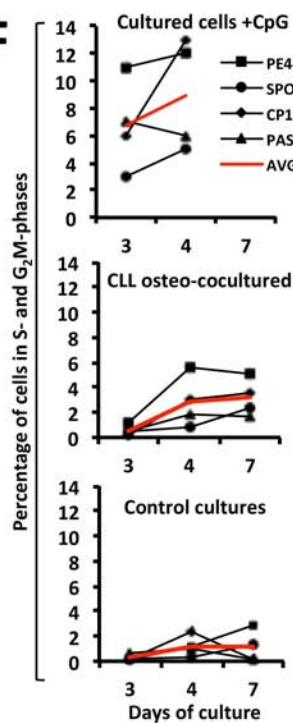


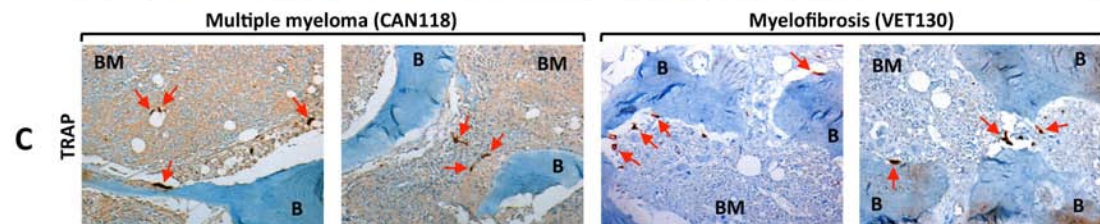
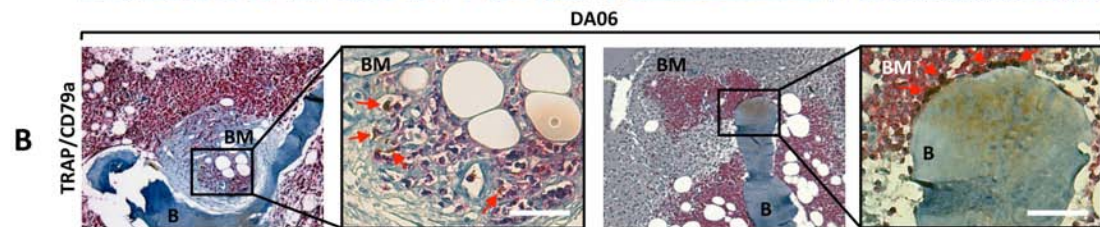
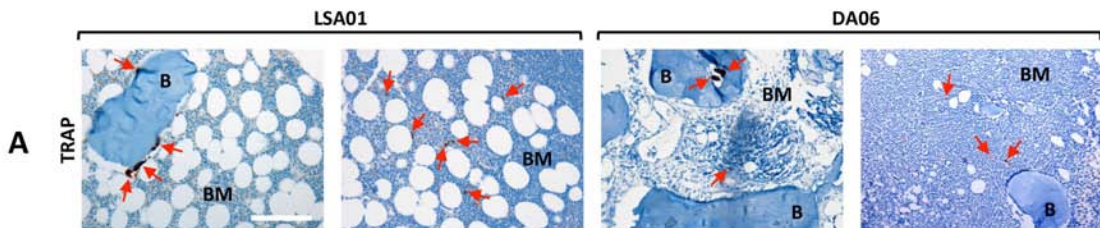
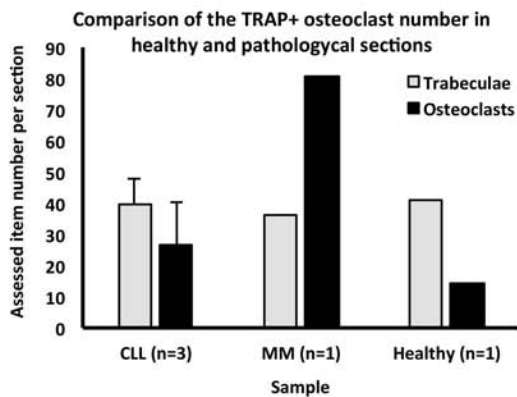
## C Reduction of CLL-cm increased osteoclastogenesis by Infliximab



## D Determination of TNF $\alpha$ (n = 6)



**A****B****C****D****E****F**

**A****B**

## Supplementary Materials and Methods

### Patients.

Forty-five patients were enrolled in the present study (Binet stage: 19A, 17B and 9C; 19 female and 26 male with a mean age  $\pm$  SD of  $69 \pm 10$  years) including subjects already examined in a previous work (Marini C, et al.; Scientific reports. 2017; 7(1):14159). Peripheral blood and sera were collected after informed consent and the study has been approved by the Ethics Committee of IRCCS Policlinic San Martino Hospital. Patients studied in GEP analysis were 217 newly diagnosed CLL cases (early stage Binet A) prospectively enrolled from several Italian institutions in an observational multicenter study (clinicaltrials.gov#NCT00917540) as previously described (Ronchetti D et al.; BMC MED Genomics 2013; 6:27-37; Ronchetti D et al.; Blood Cancer Journal, 2016; 6(9):e468). The MEC-1 cell line (obtained from DSMZ Cell Line Collection, Germany) was used in some selected experiments. All experiments were performed in accordance with relevant guidelines and regulations.

### Preparation of conditioned media from CLL cells cultures and of sera.

Conditioned media were prepared by culturing  $1 \times 10^6$  CLL cells/well/ml (24 well plate) for 72h in RPMI 1640 medium with 10% FCS. Spent media were thus collected centrifuged, filtered and frozen at  $-20^\circ\text{C}$  until further use. Sera from CLL patients were prepared from blood samples following standard procedures and frozen at  $-20^\circ\text{C}$  until use.

### *In vitro* generation of osteoblasts from BMSC.

Purchased Bone marrow stromal cells (BMSC; Lonza, Walkersville, MD, USA) were seeded at the concentration of  $8 \times 10^6$  /plate in petri dishes and cultured in Coon's modified F12 medium (Biochrom A.G., Berlin, Germany) with 10% fetal calf serum (FCS), 1% L-glutamine, 10 ng/mL of Fibroblast Growth Factor (FGF2, Miltenyi Biotech GmbH Friederich-Ebert, Germany). Cells expanded until confluence were washed with PBS (Euroclone S.p.A., Milan, Italy), detached, pooled and plated in 24-well plates. Confluent cells were then osteogenically induced with a medium prepared by adding 200  $\mu\text{M}$  Ascorbic Acid, 10 mM  $\beta$ -Glycerophosphate and  $1.0 \times 10^{-8}$  M Dexamethasone to the standard expansion medium for 9 days.  $1 \times 10^6$  of CLL B cells (in contact or in transwell), CLL cell conditioned media (CLL-cm: 200  $\mu\text{l}$ ) or CLL sera (CLL-sr: 200  $\mu\text{l}$ ) were added to differentiating osteoblasts by replacing an equivalent volume of osteogenic medium. Triplicate samples were prepared for each condition and maintained for 5 more days: osteoinduced BMSC were then detached, collected and processed for further RNA analyses (supplementary Figure 1).

### Messenger RNA extraction, reverse transcription and quantitative real time RT-PCR.

Messenger RNA was extracted by using the PerfectPure RNA Cultured Cell Kit (5-Prime GmbH, Hamburg, Germany), according to the manufacturer's instructions. Sample pools of cDNA were generated using the SuperScript<sup>TM</sup> III First-strand synthesis system for RT-PCR Kit (Invitrogen; Milan, Italy). The relative expression of the target genes was assessed by sybr-green real time quantitative RT-PCR by using the RealMasterMix SYBR ROX 2,5X (5'-Prime) in an Eppendorf Mastecycler Realplex<sup>2</sup> apparatus; quadruplicate reactions were performed for each sample, applying the following

settings: a denaturation single step at 95°C for 3 minutes; 35 cycles at 94°C for 30 sec, 60°C for 30 sec, 72°C for 40 sec, and a final step at 72°C for 7 min. The melting curve analysis was used to determine the specificity of reaction. The expression of each gene was normalized to the endogenous control gene GAPDH; primer sets for target genes were derived from published sequences (glyceraldehyde-3-phosphate dehydrogenase, GAPDH; RUNX2; Osteopontin, OP; Osteocalcin, OC (Shyti G., et al.; *Int J Artif Organs*, 2014, 37-149-154; Narcisi R., et al., *J Cell Physiol*, 2012, 227:3282-3290); or purposely designed (Dkkopf-1, DKK-1; forward primer: CGGGAATTACTGCAAAAATGGA; reverse primer: GCACAGTCTGATGACCGGAGA; Cathepsin K, Cat-K, forward primer: TCCTTCCAGTTTTACAGCAAAG, reverse primer: GTTTCCCCAGTTTTCTCCCC; NFAT-1, forward primer: TGCAACGGGAAGAGAAAGCG, reverse primer: GTCTTGGGAGAGGACTTAACC; Matrix Metalloproteinase 9, MMP9, forward primer: ACTGAGGAATGATCTAAGCCC; reverse primer: TCGAACTTTGACAGCGACAAG). Expression levels in osteogenically-induced BMSC control cultures were set as reference for further normalization among different samples and/or culture conditions.

### **Short-interfering RNA-mediated knock-down of specific cytokines in MEC-1 cell line or CLL cells**

All short-interfering RNAs (siRNA), whether IL-6-, IL-11- or TNF $\alpha$ -specific (GeneSolution siRNA, Cat. n. 1027416; products: HS\_IL6\_1,2,5,6; Hs\_IL11\_4,5,6,7; Hs\_TNF\_1-2-3-5, respectively) or aspecific (FlexiTube siRNA, AllStars Negative controls, cat. N. 1027415) were purchased from Qiagen (Qiagen s.r.l., Milano, Italy) and used at a final concentration of 80 nM. Aliquots of  $1.5 \times 10^6$  cells, either MEC-1 or BA 101, were washed with PBS and cultured in standard RPMI medium in the absence of antibiotics and low serum concentration (5%) for 24 hours, prior to transfection. Transfections were performed by using Lipofectamine 2000 (Invitrogen-Life Technologies; cat. N. 11668-019), diluting siRNAs and Lipofectamine in Opti-MEM Reduced Serum Medium (GIBCO, cat. N. 11058-21) according to the siRNA manufacturer's instructions. Cells were exposed to the siRNA-Lipofectamine complexes in the same medium at 37°C, under gentle rocking, for the subsequent 6 hours. Fresh RPMI medium+5% serum was then replenished and transfected cells maintained in standard culture conditions. After 72 h conditioned medium of cells, knocked-down for each specific cytokine, was collected, aliquoted and stored at -20 C° until further use. TNF $\alpha$ , IL-11 and IL-6 levels in the recovered conditioned media were assessed by ELISA, as subsequently indicated. SiRNAted-cells were also processed to determine the efficacy of the cytokine knock-down procedures through cytofluorographic analysis after intracytoplasmic staining with a PE-conjugated anti-TNF $\alpha$  moAb (Immunotools, Friesoythe, Germany).

### **Evaluation of matrix deposition by osteo-induced BMSC through Alizarine Red staining.**

Osteogenically-induced BMSC were cultured in different conditions as above described. In selected experiments neutralizing anti-TNF $\alpha$  and an anti-IL-6R moAbs (Infliximab, and Tocilizumab both kind gifts from Dr. Puppo, IRCCS- Policlinic San Martino Hospital, Genoa, Italy; 200  $\mu$ g/mL and 10  $\mu$ g/mL, respectively), anti-IL-11 (AF218, RD systems, Minneapolis. MN USA; 0.5  $\mu$ g/mL) or the anti-GP130 moAbs (MAB628 clone 28105, RD Systems; 2.0  $\mu$ g/mL) or an isotypic control mouse IgG1 K (cat. N. 16-4714-85; eBioscience-Thermo Fisher Scientific, Frederick, MD, USA) were added contemporarily to CLL-cm. Wells were washed in PBS and fixed in para-formaldehyde (4% in PBS) for 15 min. Extensive PBS washings were performed after fixation, followed by a brief rinsing in tap water.

Mineral deposits were then revealed by staining culture wells with Alizarine Red S (2% in water, pH 4.3; Sigma-Aldrich, Milan, Italy) for 10 min. The dye was removed and wells were rinsed twice with absolute ethanol and dried at RT. Images of each well (at least two for each culture condition) were acquired using a Nikon Digital Sight DS-5Mc camera mounted on a Nikon SZM1000 microscope. Quantification of matrix deposition was calculated as the ratio between the Alizarine-positive area of each well, expressed in pixels, vs the total image field area.

### **Generation of osteoclasts from monocytes purified from healthy donors or CLL patients.**

Monocytes ( $1 \times 10^5$ ) purified from healthy or CLL PBMCs by conjugated anti-CD14 micro-beads (Miltenyi) were seeded in 24 well plates in medium (RPMI1640 +FCS10%) and MCSF (25ng/ml; Miltenyi) and RANKL (25ng/ml; Miltenyi) were added 1 day after. Alternatively monocytes were stimulated with only MCSF (25ng/ml) and CLL-cm. Different numbers of monocytes ( $1.3 \times 10^5$  or  $2.6 \times 10^5$  cells/well) were also used in selected experiments performed in the absence of RANKL, where indicated. 500 $\mu$ l of fresh medium together with MCSF+RANKL were replaced at day 4 while at day 7 we added suboptimal concentration of MCSF and RANKL (12,5 ng/ml) together with CLL-cm or CLL-sr (300  $\mu$ l/1ml total volume) or only medium (supplementary figure 1). 72h-Conditioned media from IL-6, IL-11 and TNF $\alpha$ - silenced MEC-1 cell line was also used in selected experiments. After 7 days, the number of osteoclasts was determined by counting Tartrate-Resistant Alkaline Phosphatase positive (TRAP<sup>+</sup>) cells on an inverted Olympus CKX-41 microscope. Triplicate samples were prepared for each culture condition and at least 6 image fields were taken for each well. TRAP<sup>+</sup> cells showing at least 3 nuclei were considered as osteoclasts. In selected experiments healthy monocytes were co-cultured with CLL cells ( $1 \times 10^6$  or  $2 \times 10^6$ /ml/24well plates) and MCSF (25ng/ml). The percentage of TRAP<sup>+</sup> cells exhibiting a small or a large size was also assessed.

Nurse-like cells were generated as previously described (11) to determine TRAP expression and bone resorption activity.

Neutralizing anti-TNF $\alpha$ , -IL-11 moAbs or anti-IL-6R or -GP130 moAbs were used in selected experiments : stimulation of monocytes was performed as above reported (MCSF+RANKL) and at day 7 we added TNF $\alpha$  (30 ng/ml), or CLL-cm together with Infliximab (200  $\mu$ g/ml), or Tocilizumab (10  $\mu$ g/ml), or anti- IL-11 (0,5  $\mu$ g/ml), or anti-GP130 (2  $\mu$ g/ml) moAbs.) When the experiments were performed in the absence of previous RANKL stimulation, we contemporarily added MCSF+CLL-cm alone with/without neutralizing moAbs. The activity of the BTK inhibitor Ibrutinib (500 nM; D.B.A. Italia S.R.L., Milan, Italy) was further tested by adding it in cultures together with CLL-cm at the time of the last stimulation. Selected experiments were also performed by adding Denosumab (Xgeva, Amgen srl, Milan, Italy). The number of osteoclasts generated for each experimental condition was determined as above described.

### **TRAP Staining.**

Purified monocytes induced to differentiate toward osteoclasts were washed in PBS and fixed for 15 min at RT with a 4% PFA in acetate/citrate buffered solution (pH 6.0). Cells were subsequently

stained according to the protocol provided with the Tartrate-resistant acid phosphatase detection kit (Sigma-Aldrich, kit. N. 387A, Milan, Italy), by exposing fixed cells to a freshly prepared tartrate-containing solution for 60 min at 37°C. The staining solution was then removed and cells were washed in distilled water and photographed. TRAP-positive cells were grouped according to their dimensions. In each image field the area of trinucleated and TRAP<sup>+</sup> cells was measured by using the public software NIH Image J (version 1.48v; <http://imagej.nih.gov/ij>) tools. The cut off size to categorize a cell as small or large was an area of 25000 pixel.

### **Bone resorption Assay.**

Determination of bone resorption activity was performed by seeding CD14<sup>+</sup> purified monocytes from healthy donors in 24 well plates coated with an inorganic crystalline material (Corning, Osteo Assay Surface multiwall plates; cat.n. CLS3987-4EA) and inducing their differentiation toward osteoclasts as above described. After 14 days cells were stripped from the plates by treatment with a 10% sodium hypochlorite solution for 10 min; wells were thoroughly washed and dried at RT for 4 hours. Images of triplicate experimental conditions were acquired and the size of resorption pits was evaluated using the public software NIH Image J. The pit size was calculated as the ratio between the area of each pit, expressed in pixels, vs the total image field area.

### **Analysis of cellular viability and of cell cycle by DiOC6 and Propidium Iodide (PI) staining respectively. Evaluation of Ki67 expression on CLL cells after co-culture with osteoclasts.**

Osteoclasts or their progenitors (small trinucleated TRAP<sup>+</sup> cells) were derived as above described. After 14 days plates with mature osteoclasts were washed with PBS and further co-cultured with 1x10<sup>6</sup> CLL cells in RPMI+FCS10%. Percentage of CLL cells in apoptosis was determined at different time points (72h, 96h, 7days) through DiOC6 staining as previously described (De Toter D., et al.; Blood; 2006;107(9):3708-3715). The expression of Ki-67 was evaluated on CLL cells before and after co-culture with osteoclasts through double staining with CD19 and Ki-67 specific moAbs and the samples were analyzed in flow cytometry by FACSCanto (BD Biosciences Pharmigen, San Jose, CA, USA). Multiparameter flow cytometric analysis of cellular viability by propidium iodide (PI) exclusion assays, and cell cycle-phase distribution by DNA content was performed as previously described (Bruno S., et al.; Leukemia. 2012; 26(10):2260-2268). Briefly, CLL cells were incubated with 0.05% Triton X-100, stained with 30 µg/ml PI+0.5 mg/ml RNase (both Sigma Chemical Co.) for 30 min and measured by flow cytometry (FACSCalibur, Becton Dickinson, San José, CA). The resulting DNA content histograms provided information on proliferation (cell-cycle-phase distributions) and apoptotic DNA fragmentation ('sub-G0/G1' region). Proliferation features are herein expressed as % of cells in S+G<sub>2</sub>M cell cycle phases (hyper diploid fraction).

The expression of Ki-67 was evaluated on CLL cells before and after co-culture with osteoclasts through double staining with CD19 and Ki-67 specific moAbs and processing samples for flow cytometry by a FACSCanto apparatus (BD Biosciences Pharmigen). Briefly, samples were stained with the anti-human CD19 fluorescein-conjugated antibody (Immunotools, Friesoythe, Germany) at 4°C for 30 min. After 3 washes with PBS cells were incubated with PFA1% for 15 min at 4°C, washed again and then incubated with Methanol for 10 min; during the last 4 min 0.1% of saponin was

further added. Following 3 washes 20 µl of FITC mouse anti-Ki-67 (Ki-67 Set BD Biosciences Europe, Erembodegem, Belgium) or its specific negative control were added together with 0.1% saponin and incubated at 4°C for 45 min. Thereafter cells were washed and analyzed.

### **Evaluation of pSTAT3 and AKT expression in osteo-induced BMSC cultured with CLL-cm in the presence/absence of neutralizing TNF alpha moAb or in osteogenic-medium only.**

Osteo-induced BMSC cultured with only medium or with CLL-cm (TM145) in the presence or absence of Infliximab for 48h were first detached, washed with PBS and incubated with PFA 1% for 15 min at 4°C, washed again and then incubated with Methanol for 10 min; during the last 4 min 0.1% of saponin was further added. Following 3 washes, 20 µl of anti-phospho-STAT3 (ser727) (Invitrogen) or of anti-AKT (Cell Signaling Technologies, Danvers, MA, USA) polyclonal antibody or a specific control were added together with 0,1% of saponin and incubated at 4°C. After 45 min of incubation and 3 washes in PBS, samples were further stained with a PE-conjugated anti-rabbit secondary antibody + 30ul of 0.1% of saponin. Thereafter cells were washed and analyzed.

### **Immuno-histochemical analyses of bone biopsies from CLL patients**

Tissue was fixed in B5 (Sigma Aldrich) for 2.5h and decalcified for 3h before processing. B5-fixed, paraffin-embedded blocks were sectioned at 2 mm, deparaffinized and rehydrated. Endogenous peroxidase was blocked with 5% H<sub>2</sub>O<sub>2</sub> for 10 min. Immunoreactions for TRAP staining (clone 26E5 Life Technologies, Monza, Italy) and CD79α staining (clone SP18, Ventana Medical Systems), were performed using the automated BenchMark Ultra XT immunostainer (Ventana Medical Systems, Arizona, USA). Standard heat-based antigen retrieval (pH 6.0) was performed for TRAP and CD79α (64 min and 36 min, respectively). The Ultraview DAB detection kit, a streptavidin–biotin-based indirect method (Ventana Medical System), was used for immunostaining at 37°C for 40 min. Therefore slides were then processed for standard mounting. Images acquired from each section were scored for TRAP+ and/or CD79a+ cells. The number of multinucleated TRAP+ cells was counted in 2 different sections from bone biopsies of 3 CLL patients (LSA01, DA06, BS13), one multiple myeloma patient and one normal control. Data are mean of the number of osteoclasts and of trabeculae of the 2 sections for each patient.

### **Detection of TNFα, IL11 or IL-6 in sera from mice grafted with CLL cells and/or in media recovered from co-cultures of osteo-induced BMSCs and CLL cells.**

An in vivo xenograft model of CLL growth has been developed in our Laboratory and loss in trabecular bone structure in the femurs of mice injected with leukemic cells has been documented (Marini C., et al.; Scientific reports. 2017;7(1):141592). Human and mouse TNFα levels present in sera collected from the same mice previously studied were measured using Millipore's Milliplex MAP human Bone Magnetic Bead Kit (HBNMAG-51k, Millipore Sigma, Burlington, MA, USA) and acquired by MAGPIX instrumentation. The levels of human TNFα present in media from CLL cells cultured alone or co-cultured with osteo-induced BMSC for 5 days were also determined by using the same kit. Levels of TNFα, IL-11 or IL-6 in conditioned media of CLL cells, *per se* or upon cytokine-knock down, were assessed by standard ELISA procedures, by using EH3TNFA (Thermo Fisher

Scientific), RAB0250A-EA Human IL-11 and RABIL6A-EA Human IL-6 detection kits (SIGMA Life Sciences), respectively.

**Comparison of the levels of TNF $\alpha$ , present in co-cultures of monocytes stimulated with MCSF+RANKL with/without conditioned media from different CLL patients.**

Comparison of the levels of TNF $\alpha$  present in co-cultures of monocytes differentiating toward osteoclasts under different conditions was further performed through a qualitative Elisa assay (Quiagen Sciences Maryland, USA) following manufacturer's instructions.

**GEP analysis.**

CD19<sup>+</sup> purified CLL samples and normal peripheral blood (PB) B cells were profiled on GeneChip Gene 1.0 ST Array (Affymetrix, Santa Clara, CA), as previously described (Morabito F., et al.; Clin Cancer Res. 2013;19(21):5890-5900). Normalized expression levels were processed by the Robust Multi-array Average procedure (Irizarry RA, et al.; Biostatistics 2003; 4:249–64.) with the re-annotated Chip Definition Files from BrainArray libraries version 19 (Dai M, et al.; Nucleic Acids Res 2005; 33:e175), available at <http://brainarray.mbni.med.umich.edu>.

**In silico interrogation of public data on human MSC co-cultured with CLL cells.**

Expression levels of selected genes (RUNX2, Collagen 1A, BMP-4, BMP-6, DKK-1, OP, Osterix, RANK, RANKL,  $\beta$ -CAT, NOTCH1, NOTCH2, OC, BMP-2, Wnt3a, Wnt5a) were extracted from GSE129108 dataset profiled on Illumina HumanHT-12 v4 Expression BeadChip (Schulze-Edinghausen L et al., Cancers 2019), comparing untreated human primary mesenchymal stromal cells (MSCs) from two different donors each of which co-cultured for 5 days with CLL cells derived from two different patients.

**Statistic.**

Two-sided Student *t*-test, U-Mann-Whitney test, or  $\chi^2$  test with Fisher's correction were used. All data sets used displayed a normal distribution; *p* values are depicted as \*, \*\* or \*\*\* for  $p \leq 0.05$ ,  $\leq 0.01$  or  $< 0.001$ , respectively.

## Legends to SUPPLEMENTARY FIGURES

**Supplementary Figure 1: Experimental models.** Here are depicted different passages employed to derive osteoblasts or osteoclasts and to assess their differentiation under the various culture conditions adopted.

**Supplementary Figure 2: Effects of the addition of neutralizing anti-cytokines moAbs to BMSC cultured with CLL-cm (TM145).** **A and B:** The addition of anti-TNF $\alpha$  or the IL6R moAbs, but not of an isotypic control moAb, induced a decrease in matrix mineralization. **C and D:** RUNX2 and Osteocalcin mRNAs levels were rescued by the addition of neutralizing moAbs to osteo-induced BMSC cultured with CLL cm (TM145). **E and F:** pSTAT3<sup>ser727</sup> and AKT were downmodulated in osteoinduced-BMSC cultured for 48h with CLL cm (TM145). The addition of anti-TNF $\alpha$  moAb however re-induced higher levels of expression similar to those of BMSC cultured in osteogenic medium only (BMSC).

**Supplementary Figure 3: Evaluation of TNF $\alpha$ , IL-11 and IL-6 levels in RNA-silenced MEC-1 cell line or leukemic CLL cells or in conditioned media from different CLL patients through immunofluorescence or Elisa assays.** **A:** Downmodulated expression of TNF $\alpha$  in siRNA-transfected MEC-1 or CLL cells (BA101), as detected by immuno-fluorescence and cytofluorographic analysis. **B, D, E, G:** Histograms evidence reduced levels of the secreted cytokines in cm from siRNA transfected cells. **C, F, H:** Discrete amounts of TNF $\alpha$ , IL-11 and IL-6 are present in CLL-cm from different CLL patients.

**Supplementary Figure 4: Gene expression profiles of IL-11 and IL-11RA in CLL cells and normal B controls.** IL-11 and IL-11RA are significantly more expressed in CLL B cells than in normal B cells of controls, as determined through GEP analysis ( $n=217$  early stage Binet A CLL cases, and  $n=6$  B control cases). Statistical significance was evaluated by the U-Mann Whitney test.

**Supplementary Figure 5: Evaluation of TNF $\alpha$  levels in media derived from CLL cells cultured alone or with osteo-induced BMSC.** Higher TNF $\alpha$  levels were detected in media derived from the 5-days cultures of CLL cells alone than after their co-culture with BMSC differentiating towards osteoblasts. BMSC: bone marrow stromal cells. Six patients were assessed (FW16, BE08, CRO7, JF12, MS15, MM13)

**Supplementary Figure 6: The addition of exogenous RANKL exploits the full maturation of committed osteoclasts precursors.** Monocytes stimulated with MCSF+CLL-cm, without RANKL, proceed toward the first step of osteoclasts differentiation (**A, B**) but do not reach terminal differentiation (**C, D**). In agreement to these observations, the anti-RANKL antibody Denosumab (1 ng/ml or 10 ng/ml, Dns) affects osteoclastogenesis only if RANKL is present (**C, D**). Red arrows indicate tri-(or more)-nucleated TRAP<sup>+</sup> cells. Bar sizes are 25 $\mu$ m and 12.5 $\mu$ m for 10X and 20X respectively.

**Supplementary Figure 7: Effects of cytokine interference on osteoclastogenesis.** Conditioned medium derived from TNF $\alpha$  siRNA knocked-down MEC-1 cells induced a weak decrease in large fully differentiated osteoclasts and an increase of small TRAP<sup>+</sup> cells, similarly to the effect caused by supplementation of an anti-TNF $\alpha$  moAb.

**Supplementary Figure 8: Increased levels of human TNF $\alpha$  were detected in mouse serum after human CLL cells engraftment.** **A:** In the CLL mouse model the levels of human TNF $\alpha$  were progressively increased from the 3<sup>rd</sup> to the 6<sup>th</sup> week, after human CLL cells injection and engraftment. **B.** Human TNF $\alpha$  concentration in NSG (Nod SCID  $\gamma$ -null) mice engrafted with CLL cells as compared to controls, at the time of sacrifice.<sup>(2)</sup>

**Supplementary Figure 9: Ibrutinib treatment inhibited increased-osteoclasts maturation due to the addition of CLL-cm.** **A:** Ibrutinib strongly affects osteoclastogenesis also when this process is enhanced by addition of CLL-cm in culture. Red arrows indicate TRAP<sup>+</sup> osteoclasts at least trinucleated. Size bar: 63 $\mu$ m (4X) and 25 $\mu$ m (10X). **B:** A statistically significant reduction of osteoclasts generation was evident under Ibrutinib treatment. Ibrutinib affected both large fully mature osteoclasts and small precursors. Histograms depict mean values  $\pm$  SD of 6 CLL cases, evaluated in 3 different experiments.

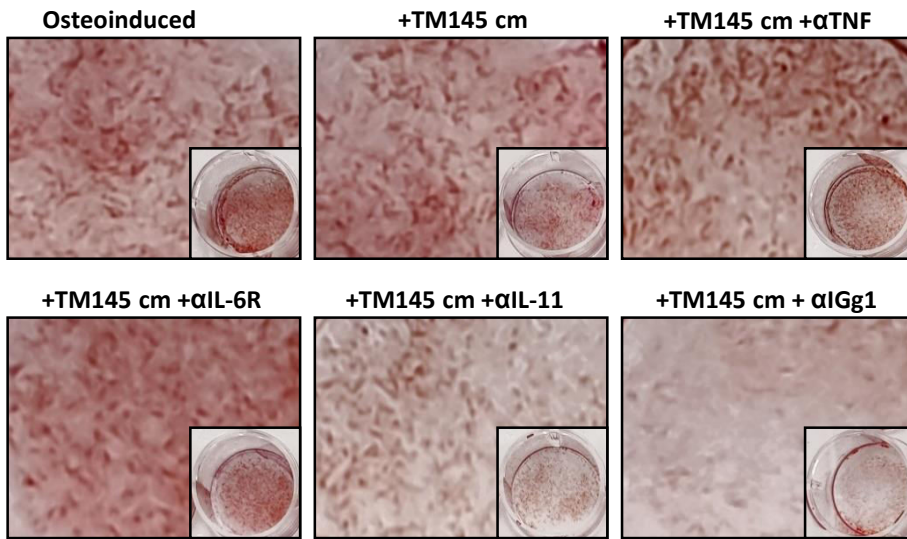
**Supplementary Figure 10: GEP of different molecules correlated to osteoblastogenesis regulation as derived from *in silico* available data.** Histograms depict significant alterations in the mean values of normalized expression levels of selected genes (RUNX2, Collagen 1A, BMP-4, BMP-6, DKK-1 and OP) in 2 MSC samples untreated or co-cultured with 2 different CLL patients for 5 days. Other analyzed targets (Osterix, RANK, RANKL,  $\beta$ -CAT, NOTCH1, NOTCH2, OC, BMP-2, Wnt3a, Wnt5a; data not presented) did not show significant modulations.

**Supplementary Figure 11: Correlation between IGVH status of CLL patients and CLL-cm-driven formation of trinucleated TRAP<sup>+</sup> cells.** Histograms depict, as fold increase, the number of trinucleated TRAP<sup>+</sup> cells obtained when pre-activated monocytes are cultured with CLL-derived cm, with respect to non-cm exposed controls; values higher than 1.25-fold significantly correlate with cm derived from unmutated IGVH patients ( $\chi^2$  test,  $p=0.0147$ ).

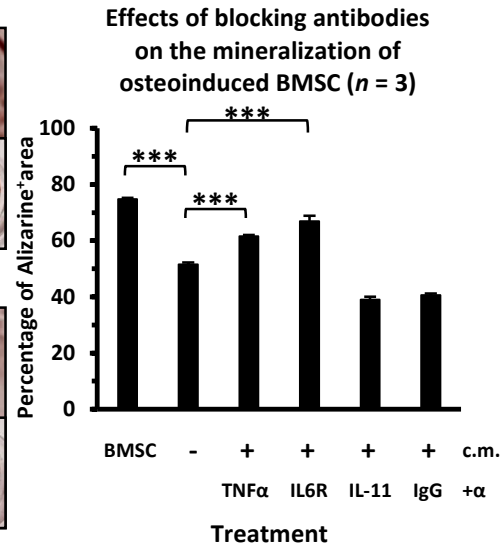


# Supplementary Figure 2

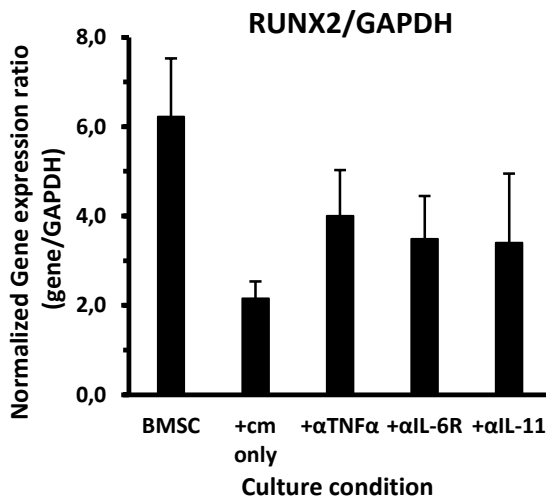
## A



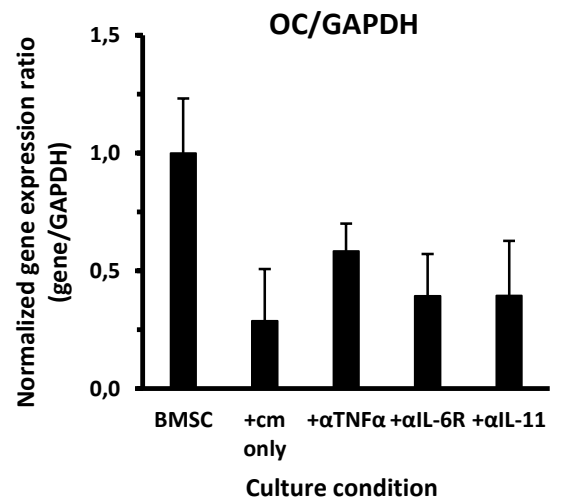
## B



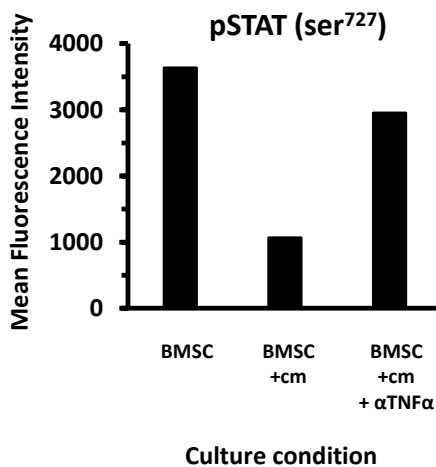
## C



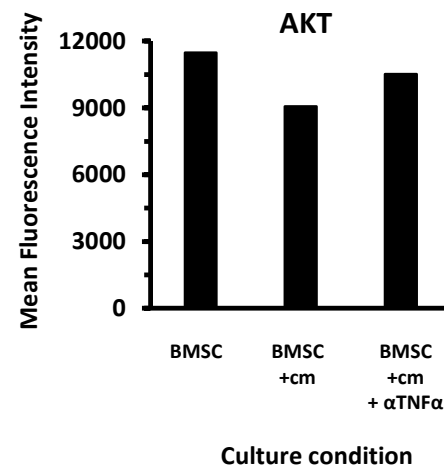
## D



## E



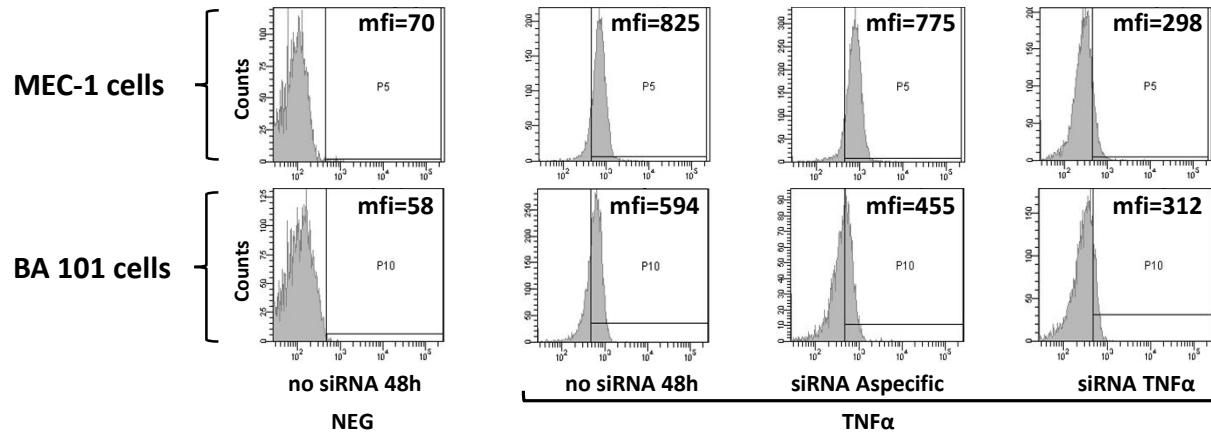
## F



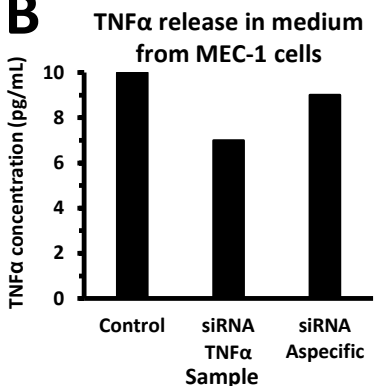
# Supplementary Figure 3

**A**

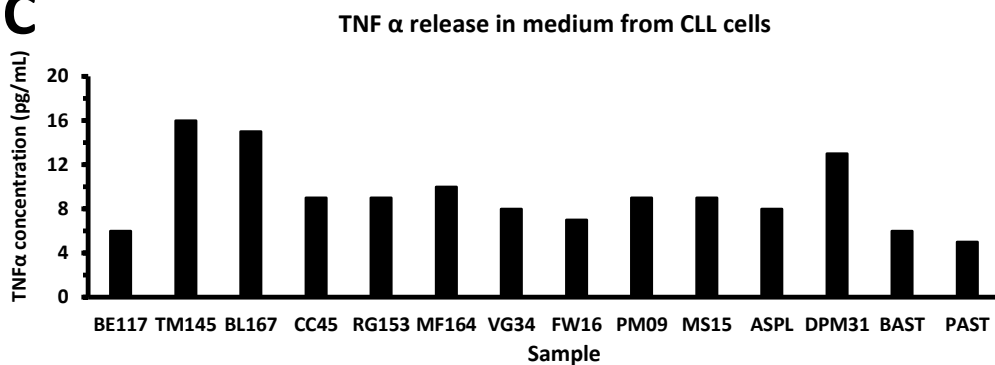
TNF $\alpha$  expression on MEC-1 and BA 101 CLL cells before and after silencing with aspecific/specific siRNA



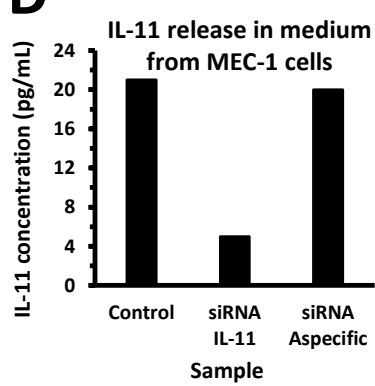
**B**



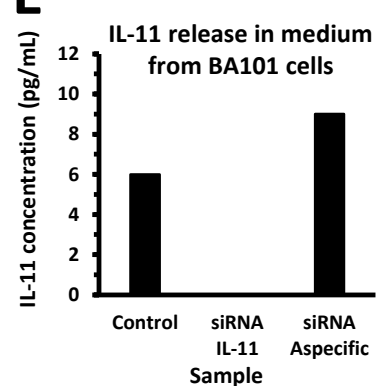
**C**



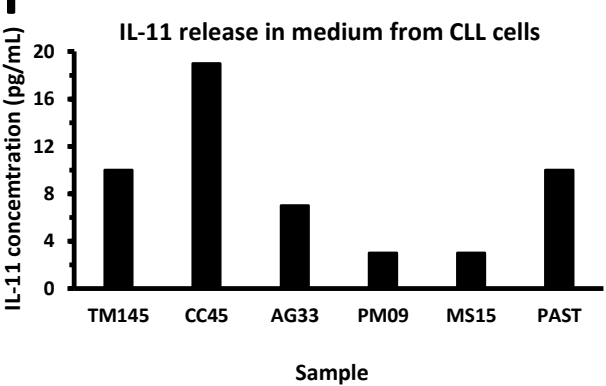
**D**



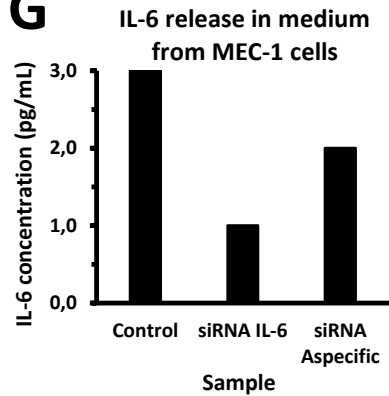
**E**



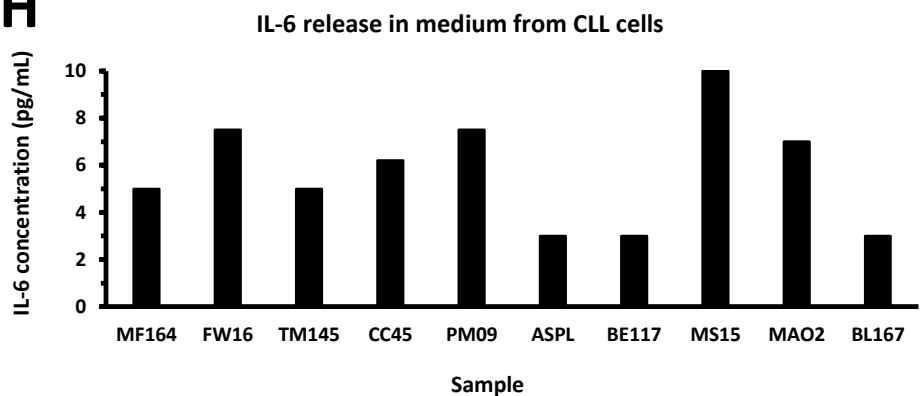
**F**



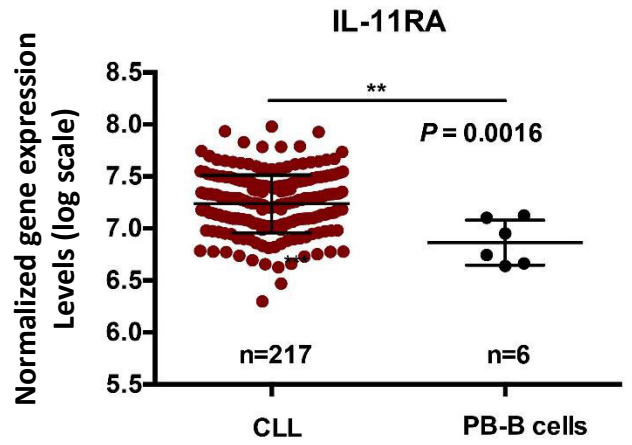
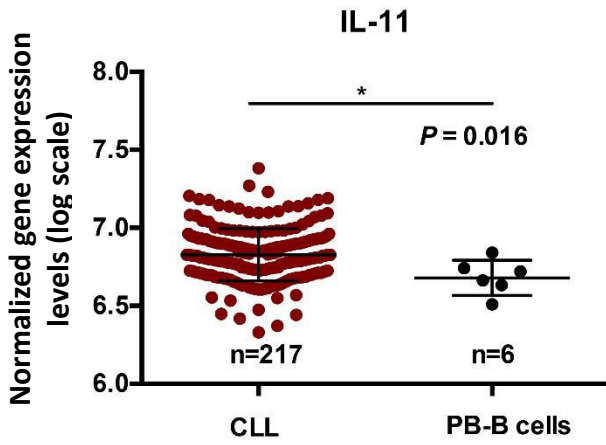
**G**



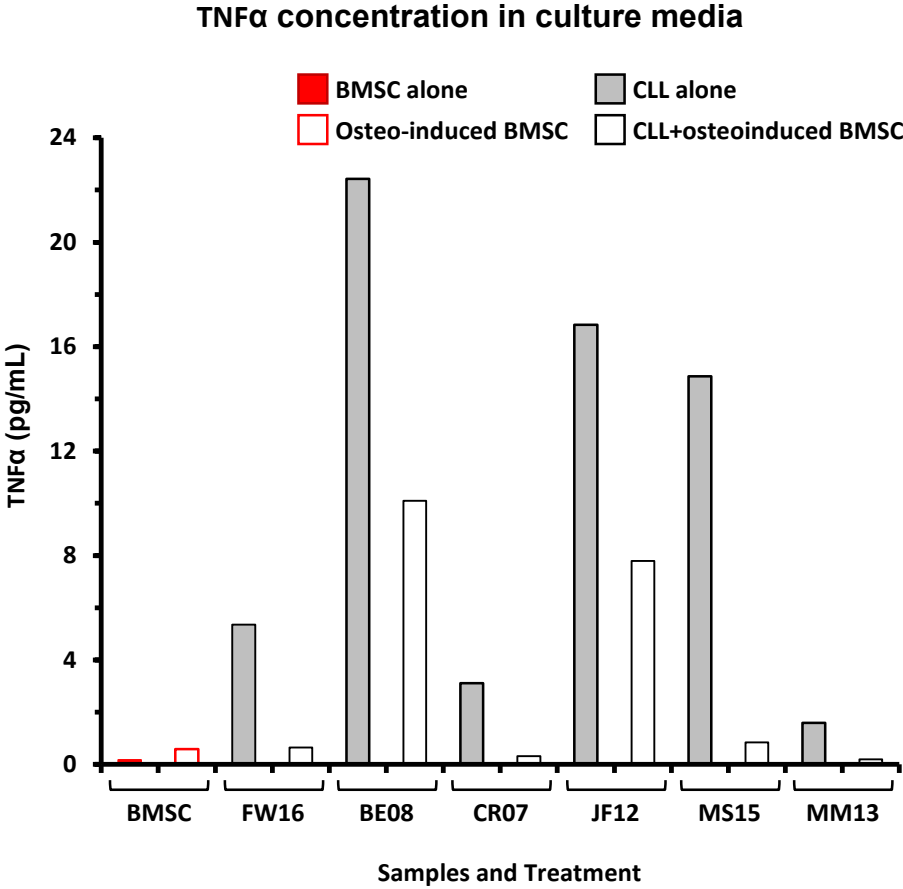
**H**



## Supplementary Figure 4

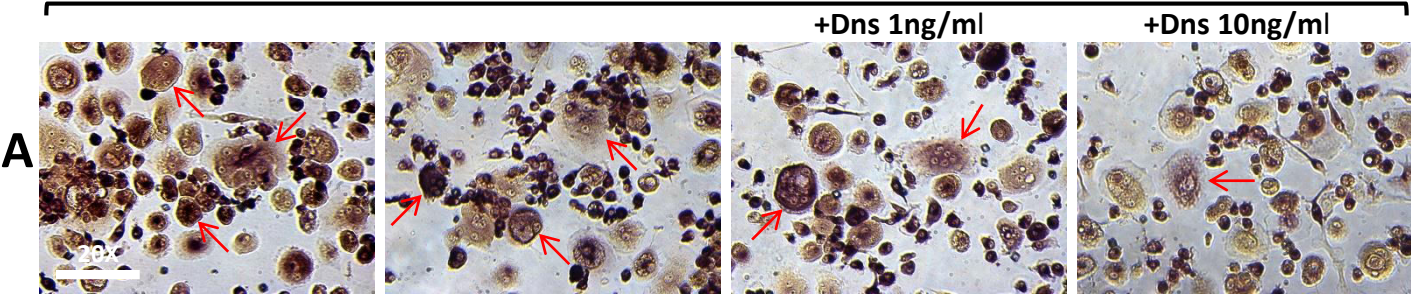


# Supplementary Figure 5

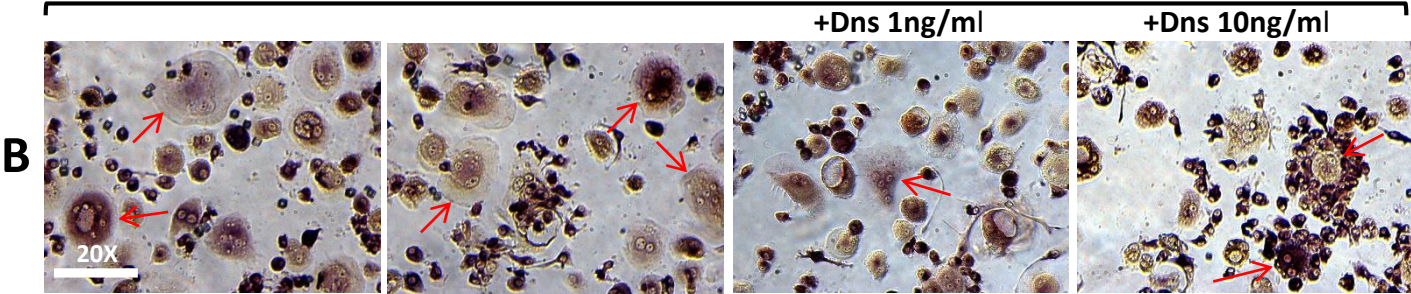


# Supplementary Figure 6

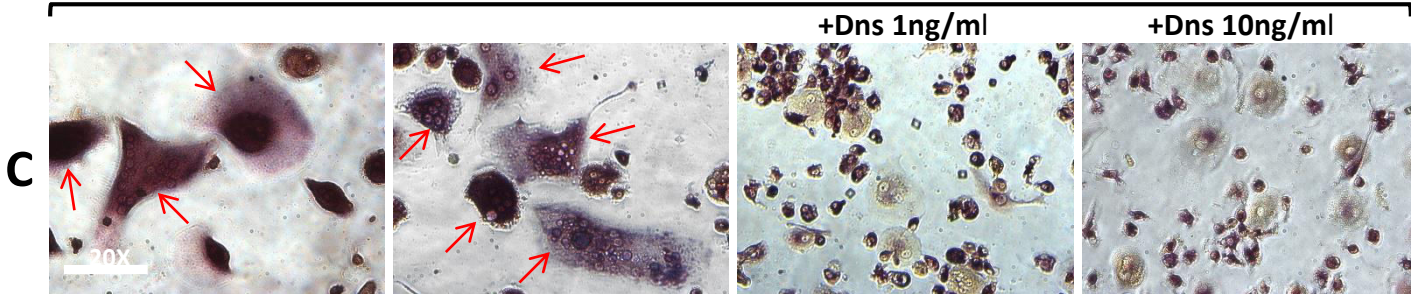
MCSF+TC38cm



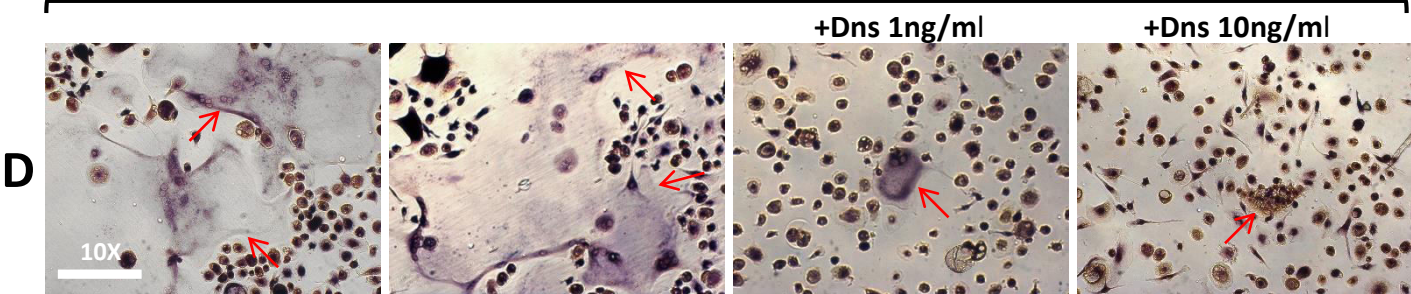
MCSF+SD36cm



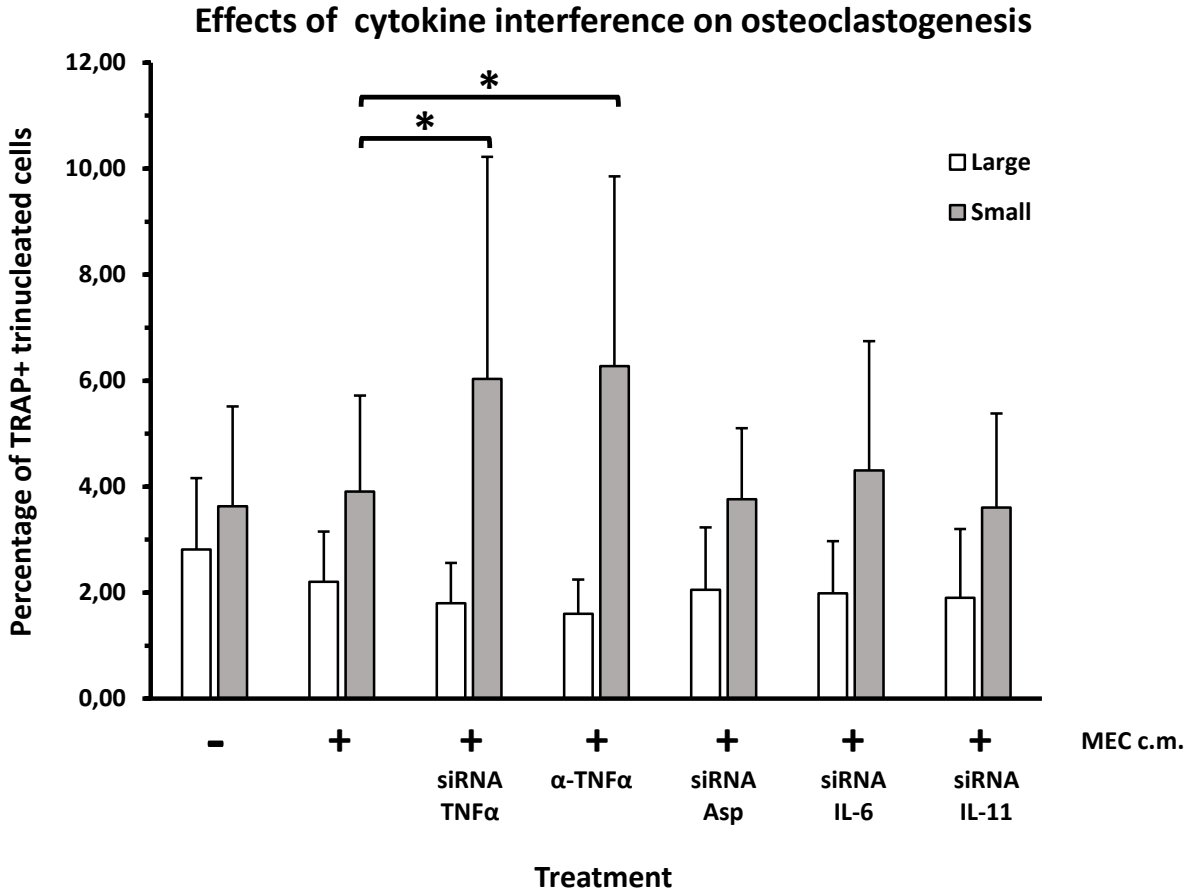
MCSF+RANKL



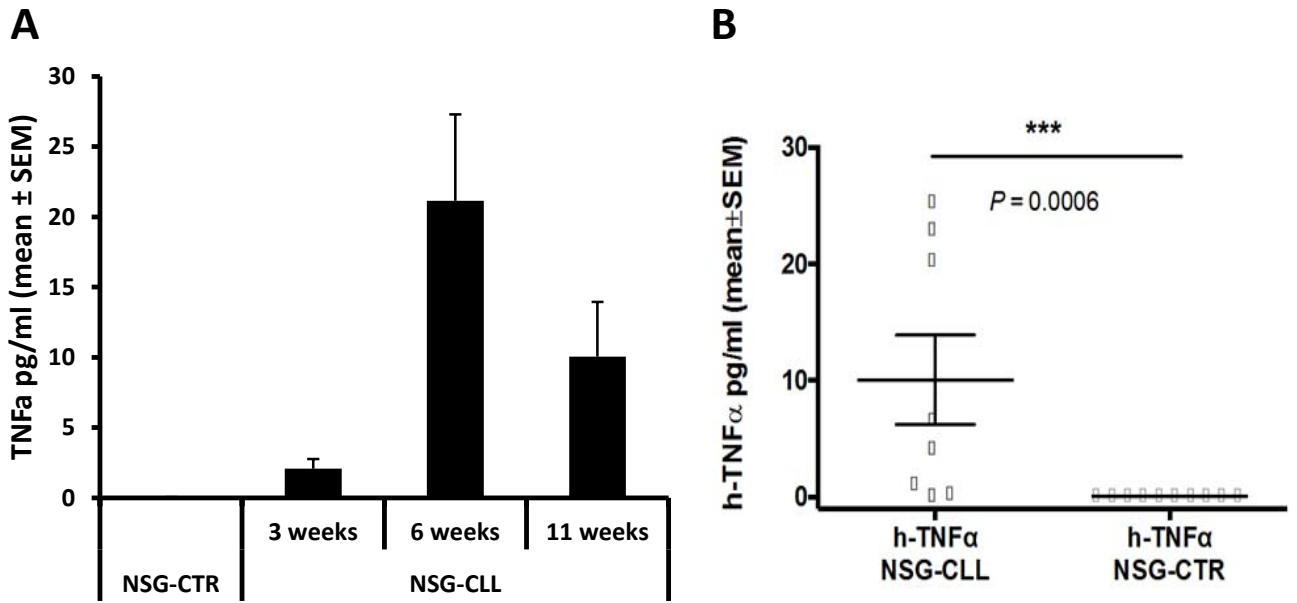
MCSF+RANKL+FW16cm



# Supplementary Figure 7

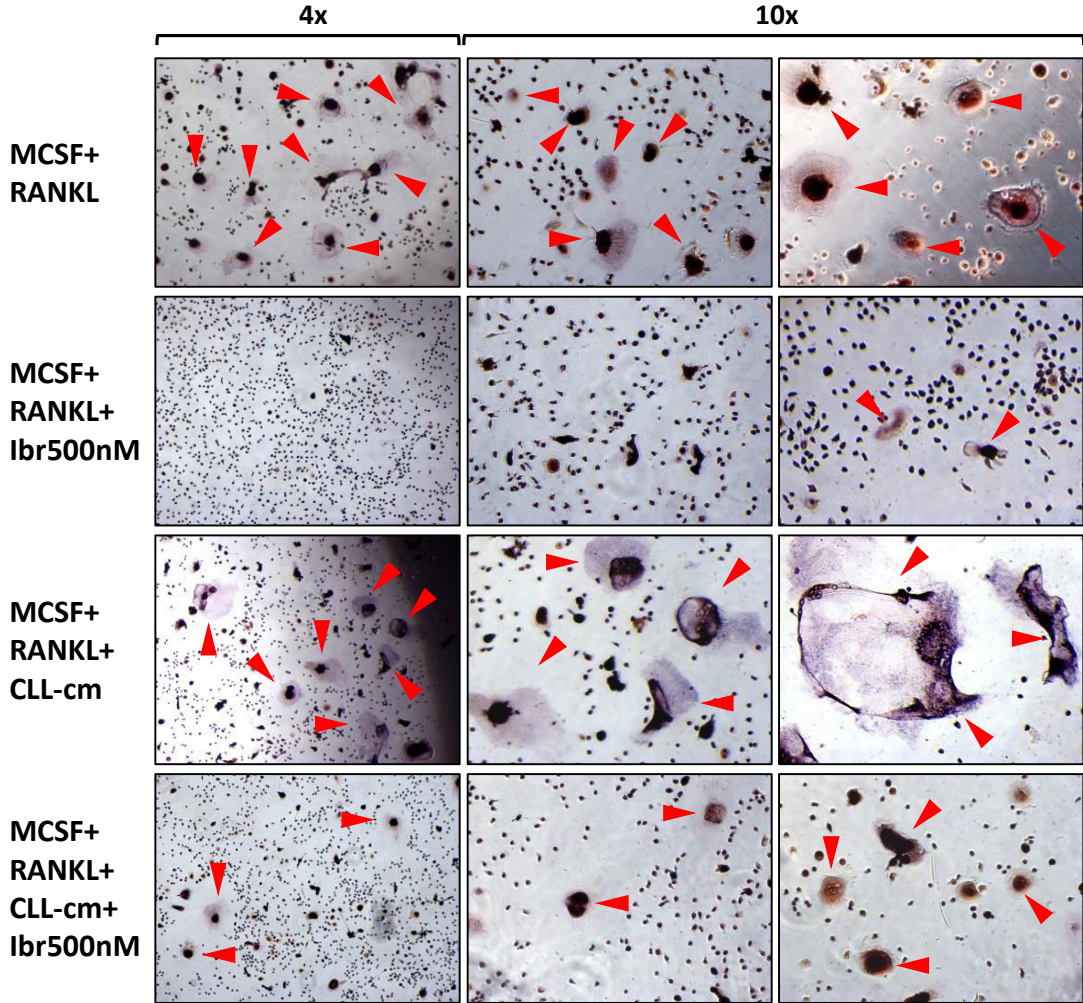


## Supplementary Figure 8

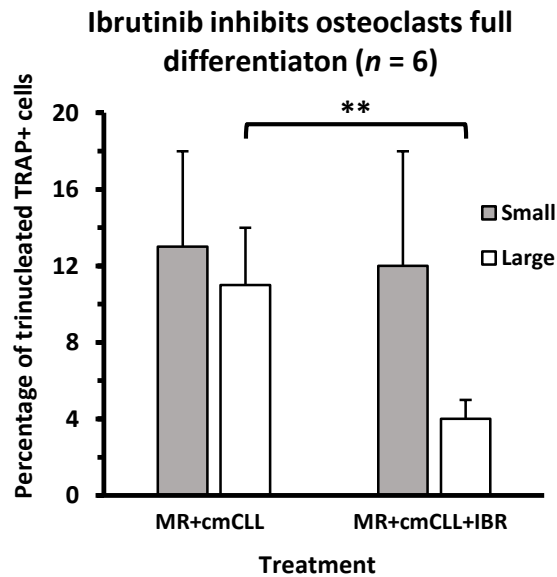


# Supplementary Figure 9

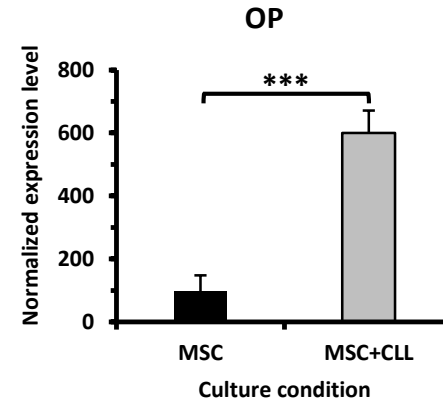
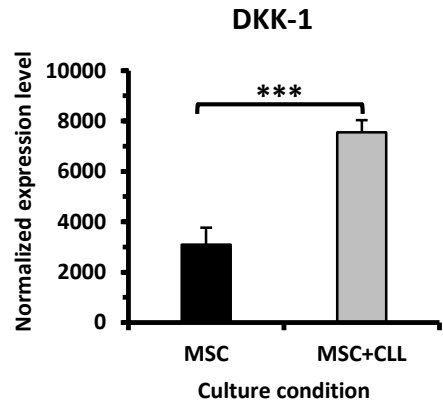
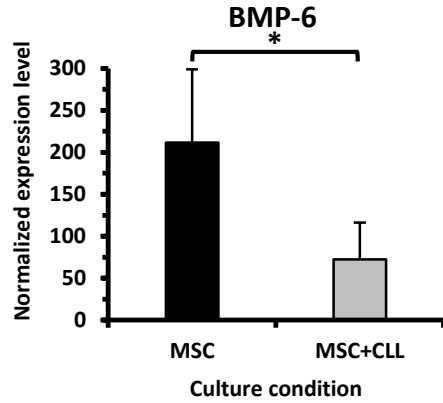
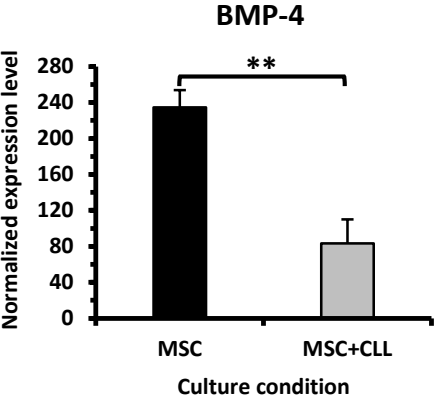
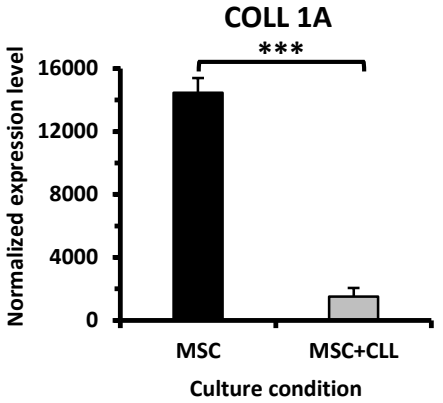
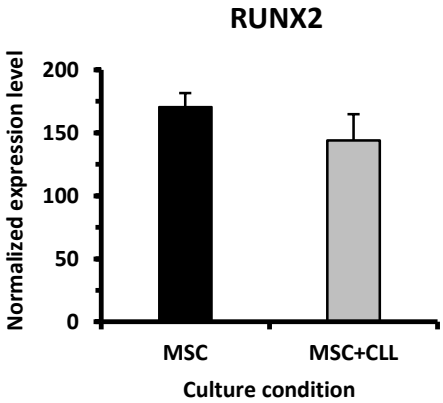
## A



## B



Supplementary Figure 10



# Supplementary Figure 11

Increased number of trinucleated TRAP+ cells correlates with IgVH status (for  $y > 1.25$  and  $n = 22$ ,  $\chi^2$  test p value = 0.0147)

